Iraqi Journal of Oil & Gas Research

Journal homepage: https://ijogr.uotechnology.edu.iq

Oil and Gas Fields Development: Well Spacing Impact on Reservoir Performance Depleted by Multiple Horizontal Wellbores

***Salam Al-Rbeawi*[1, *] *and Fadhil S Kadhim*[2]**

[1]Cyprus Metu-Northern Cyprus Campus
[2]Oil and Gas Engineering Department, University of Technology-Iraq, Baghdad-Iraq

Article information

Article history:
Received: February, 24, 2023
Accepted: March, 26, 2023
Available online: April, 08, 2023

Keywords:
Well Spacing,
Horizontal wells,
Pressure behavior,
Productivity index

Corresponding Author:
Al-Rbeawi, Salam
salam@metu.edu.tr

Abstract

This paper focuses an insight on the impact of well spacing on the performance of oil and gas reservoirs depleted by multiple horizontal wellbores distributed parallelly or radially in rectangular and circular drainage areas. The objective is to develop an integrated approach for predicting the pressure, flow regimes, flow rate, cumulative production behavior, and estimating the transient and stabilized pseudo-steady state productivity index. The motivation is eliminating the uncertainties in predicting these key parameters that are importantly used in the development plans of the reservoirs.

The methodology used in this approach consists of different tasks. The first is developing analytical models for the pressure drop, pressure derivative, and productivity index caused by a constant sandface flow rate and a constant production rate from each wellbore. The second is developing analytical models for the flow rate, cumulative production, and productivity index caused by a constant bottom hole flowing pressure. These models consider three oil and gas reservoir configurations of different boundary systems, rectangular, square, and circular-shaped drainage areas. These reservoirs are depleted by multiple horizontal wellbores of different lengths that are parallelly or radially extended in the porous media. While the third is developing pressure behavior models for pseudo-steady state flow conditions when the production pulse reaches the boundaries. The fourth task concentrates on the models of the transient and stabilized pseudo-steady state productivity index assuming that the flow rate of each wellbore does not progressively deteriorate by the near-wellbore conditions. While the fifth task demonstrates the impact of the well spacing on the productivity index of different reservoirs. The results

of the developed models are verified by the comparison with the results obtained by the state-of-the-art numerical simulators.

The outcomes of this study can be summarized in the following points: 1) Well spacing does have a significant influence on the performance of all reservoir configurations, however, it is not seen at early production time while it is very clearly observed at late production time. 2) The

impact of well spacing on radially distributed wellbores at circular drainage areas is more than parallelly and radially distributed transient state flow regime. 4) The well interference could be seen early when the well spacing is narrow. It could be observed during intermediate production time. 5) The pressure drop and the productivity index may change significantly after the well interference more than before.

wellbores in rectangular reservoirs. 3) The well spacing causes a well interference that could be characterized by developing a new flow regime called early pseudo-steady state flow that is typically followed by a

Two novel points have been found out in this study. The first is the possibility of reaching the stabilized productivity index before pseudo-steady state flow conditions due to developing an early pseudo-steady state flow regime. The second confirms the fact that increasing the number of the wellbore or decreasing the well spacing may not improve the reservoir performance.

DOI: http://doi.org/10.55699/ijogr.2023.0301.1038, Oil and Gas Engineering Department, University of Technology-Iraq

1. Introduction

Well spacing, sometimes it is called well density, is one of the key parameters of developing oil and gas fields. Technically, it affects some of the important development indicators such as the number and location of the wells that are required to be drilled, oil and gas production rate, ultimate recovery and recovery factor, and reservoir production life. Economically, it impacts the total investment represented by the capital expenditures (the cost of drilling, completion, workover, … etc.) and the total revenue. It refers, technically, to a part of a drainage area that could be produced by a single well without the interference with other nearby wells while, economically, it refers to the same part of the drainage area where the oil and gas production could give maximum net present value (NPV). It was defined for the first time by Barlow and Berwald 1945 [1] as the calculated number of acres per a well that could give the maximum economic return from the development of a reservoir as a whole under known and assumed conditions used in the calculations. Harrison 1970 [2] redefined well spacing as the distance between wells or the amount of the surface area attributable to each well while defined the optimum well spacing as the maximum number of reservoir acres that would be economically and effectively drained by one well within a reasonable time.

Not only now, well spacing has been one of the controversial topics in the petroleum industry. The reason for that is the interaction between two different approaches wherein the well spacing is a key parameter in both of them. The first is the engineering point of view in which the well spacing should be determined based on the technical aspects related to the reservoir conditions and wellbore types such as the permeability, porosity, saturation, oil or gas initially in place and the time required for depleting the reservoirs. While the second is the landlords and operators' point of view in which the well spacing should be determined based on the economic aspects such as the net return per acre. At the very early days of the oil and gas industry, there was a belief that increasing the number of the wells and decreasing the well spacing could increase the ultimate recovery. However, Cutler 1924 [3] studied the production data of several USA oil and gas fields and reached a tentative rule that said "The ultimate production for wells of equal size in the same pool (reservoir) where there is interference, shown by a difference in the production decline curves for different spacing, seems approximately to vary directly with the square root of the area drained by a well". The tentative rule presented by Cutler 1924 [3] was hardly to be accepted by all, Haseman 1930 [4] introduced "The well method for producing oil" approach that stated that four wells drilled in 160 acres of a reservoir would yield approximately four times the amount of oil produced by a single well. This approach stated also that the yield of oil per well is not always directly proportional to the number of the wells because the interference of the offset wells substantially affects the yield per well. The same conclusion was drawn by Phelps 1929 [5] who said that the spacing of 5.0-5.1 acres/well would give the maximum net return per acre and more than that would bring but very little less than the maximum net return. A few years later, Foley 1938 [6] stated that many people still have held the idea that the closer spacing among wells, the greater recovery that can be obtained, but he confirmed that this statement is not always true as the recovery is not determined by the well spacing only and a lot of parameters should be considered such as the drive mechanism and the volume of oil and gas initially in place as well as the recoverable reserve.

The debate about the well spacing had never stopped at that time, Muskat 1940 [7] introduced some of the principles that could be used for determining the well spacing in different reservoirs. He emphasized that no one could evaluate the significance of the economics of any reservoir without considering the technical aspects related to the inherent characteristics of these reservoirs. It is also equally certain that no one could reasonably predict identical ultimate recovery of two reservoirs having the same well spacing without considering the reservoir conditions. The impact of well interference caused by well spacing has been explained by Elliot 1951 [8] who concluded that wider spacing is required for preventing the well interference. He suggested that well spacing may be more than 40 acres per well, however, he had not ignored the impact of the economic considerations on the well spacing. The same concept had been reached by Craze 1958 [9] after studying the gas production from 40 fields in Texas, USA during 1957. He stated that 30% of those fields are developed with 640 acres well spacing while 57.5% are developed with 320 acres well spacing while only 12.5% are developed with 160 acres well spacing. The abovementioned well spacing by Craze 1958 [9] was approved by the Railroad Commission in Texas, USA, while 320 acres well spacing of gas-producing reservoirs was approved in Mississippi, USA. Miller and Dyes 1959 [10] emphasized that the well spacing could be influenced by reservoir type and reservoir fluid properties. They stated that the well spacing could change significantly from wide spacing for the operation at high production rates of viscous and low gravity oil in thin formation to narrow spacing in thick formations.

As a matter of fact, the debate of the well spacing had not reached a clear answer for the questions about the optimum well spacing and the ultimate recovery. In fact, according to Muskat 1940 [7] and Barlow and Berwald 1945 [1], it is not a simple problem that could be solved by a direct solution using either analytical or statistical approaches. The reason for that is the missing interaction between the key parameters of the two points of view; the economics-related parameters and the engineering-related parameters represented by the reservoir technical characteristics. Accordingly, the only conclusion that had been reached at that time after the abovementioned debate was "similar well spacing may give different recoveries and similar recoveries might be obtained from different well spacing". Because of that, not too much was said during the 1960s and 1970s and no significant and novel approaches were introduced about the well spacing. For example, Heuer and Dew 1961 [11] stated that the substantial total oil recovery from 80 acres well spacing is similar to that obtained from 40 acres spacing at the economic limit with a double time required for the production. While Chacon 1973 [12] presented a correlation for determining the optimal well spacing for the gas reservoirs of Mexico based on the production data of 20 years. He considered four variables only; the original gas in place, the gas classification, the number of the wells, and the time of exploitation.

Early 1990s, the well spacing topic had been brought back to the discussion with the growth of the hydraulic fracturing completion, multilateral horizontal wells, infill drilling, and fishbone-type completion. These development plans were significantly affected by and affected on the well spacing. The new debate had started not only about the impact of well spacing on the productivity of vertical wells but also between horizontal wellbores used for depleting oil and gas reservoirs as well as the cluster and fracture spacing in unconventional reservoirs developed by multiple hydraulic fractures. Accordingly, the interference phenomena have become a key factor in determining the well spacing. For example, using a very close spacing between parent wells (hydraulically fractured offset wells) and hydraulically fractured child wells may lead to the "frac-hit" that in turn leads to a sharp decline in the production capacity Bommer et al. 2017 [13].

The optimum positions of multiple wells producing at constant and different wellbore bottom hole flowing pressures have been discussed by Camacho-V & Galindo-Nava, 1996 [14]. They have concluded that the optimum position is a function of time if different bottom hole pressures are used, otherwise, the position is fixed. Four years later, Valko et al. 2000 [15] re-considered the impact of well positions and well spacing on the stabilized pseudo-steady state productivity index. They developed an analytical approach that could fit a moderate number of wells in a fairly homogenous drainage area. At the same time, Umnuayponwiwat et al. 2000 [16] studied the effects of different vertical and horizontal wells in closed rectangular reservoirs on the pressure behaviors and the inflow performance relationships with a consideration given to the time-variant flow rates. The inflow performance relationship of multilateral wells extended in different directions and horizons considering different spacing was developed by Guo et al. 2008 [17].

Unfortunately, unlike the impact of well spacing on the performance of hydraulically fractured reservoirs, there is very limited contribution in the literature that focuses on the impact of well spacing between horizontal wells. He et al. 2010 [18] stated that the optimum well spacing in tight sandstone gas reservoirs could be determined based on the available data taken from the 3D geological model, gas production, cumulative gas production, reservoir configuration, and the economic aspects represented by the total investments and the expected net present value. Wilson 2016 [19] analyzed the data presented by Suarez and Pichon 2016 [20] about the completion and well spacing of horizontal wells in the pad development of the Vaca Muerta Shale reservoir, the second largest gas shale in Argentina. Wilson has summed up his analysis by confirming the fact that increasing well spacing could improve the production capacity of an individual well, but it could also reduce the total production capacity from the reservoirs by reducing the number of the wells. Sahai et al 2012 [21] used the production data taken from 100 wells in Haynesville shale and 300 wells in Marcellus shale in the USA to study the impact of well spacing and determine the optimal spacing. While Zhu et al. 2017 [22] used reservoir simulation models and the available data from the lower Spraberry shale, Midland, USA, to study the impact of the well spacing on the estimated ultimate recovery (EUR). Bansal et al. 2018 [23] concluded that it is difficult to know what would be the optimal well spacing without understanding profoundly the characteristics of the reservoirs. An approach for the impact of the parent-child wellbore spacing on the pressure behavior and productivity index has been introduced by Al-Rbeawi 2020 [24] who stated that the expectations for increasing the productivity index with narrowing the wellbore spacing might be restricted by the interference between the adjacent wellbores.

This paper introduces an integrated study for the influences of the wellbore spacing on the pressure, flow regimes, flow rate, cumulative production, and transient and stabilized pseudo-steady state productivity index. The targets are reservoirs with rectangular and circular drainage areas that are depleted by multiple horizontal wells. The study has not considered the economic parameters and focused on the technical parameters only such as reservoir configuration, wellbore type and length, wellbore distribution. For this purpose, different analytical models are developed and presented in this paper for the pressure distribution and declining flow rate during the entire production life of the reservoirs. These models are simplified for the pseudo-steady state flow conditions when the production pulse has already reached reservoir boundaries and stabilized pseudo-steady state productivity index models are generated. The effect of wellbore spacing is introduced to these models and the productivity index is calculated for different reservoir configurations and wellbore types and distributions.

2. The impact of well spacing on pressure and production behavior

For a rectangular bounded reservoir with two side boundaries (x_e), and (y_e) depleted by parallelly distributed wellbores as it is shown in Fig. (1a) or depleted by radially distributed multilateral wellbores as it is shown in Fig. (1b), the pressure drop, in dimensionless form, caused by a constant production rate of a single horizontal wellbore of half-length (L_w) is given by:

$$P_{wD} = P_D + (P_{ND} + s_m) \tag{1}$$

While the dimensionless pressure drop caused by the production from multiple horizontal wellbores (N) producing the same and constant flow rate is given by:

$$P_{wDj} = \sum_{j=1}^{j=N} P_{Dj}\, q_{Dj} + \left(P_{NDj} + s_{mj}\right) q_{Dj} \tag{2}$$

The production rate behavior with time, in dimensionless form, assuming a constant bottom hole flowing pressure can be determined using Duhamel's formula [25]:

$$q_{Dj} = \mathcal{L}^{-1}\left(\frac{1}{s^2 \overline{P_{wDj}}}\right) \tag{3}$$

while the cumulative production, in dimensionless form, is determined by [26]:

$$N_{Dj} = \mathcal{L}^{-1}\left(\frac{1}{s^3 \overline{P_{wDj}}}\right) \tag{4}$$

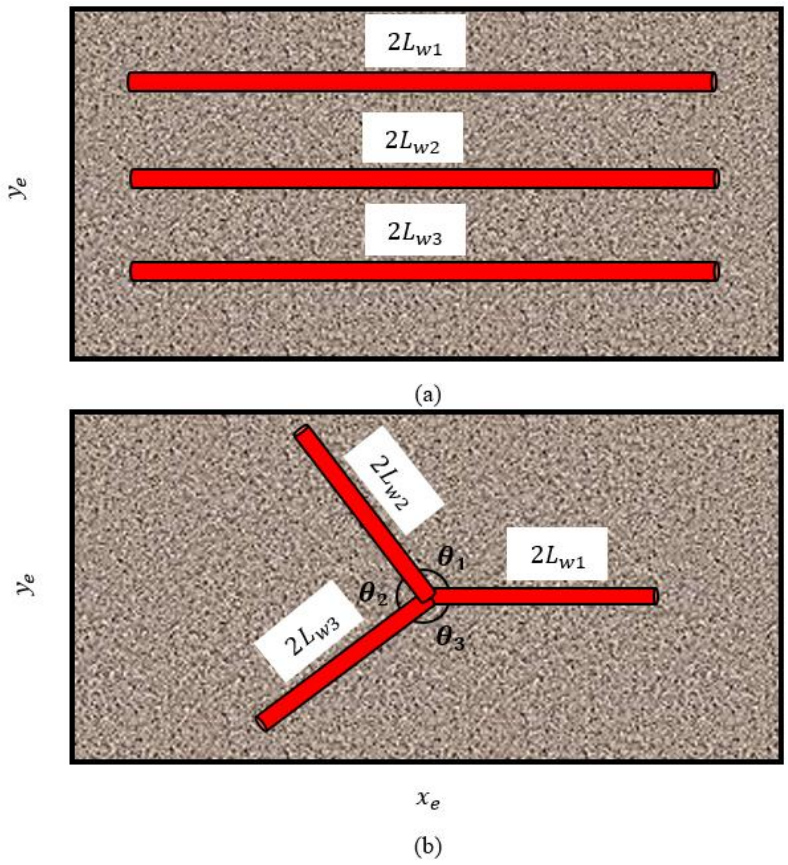

Figure 1: Rectangular bounded reservoir with multiple horizontal wells (a) Parallelly distributed wellbores (b) Radial distributed wellbores.

Eq. (1) suggests that the total bottom hole pressure drop (P_{wD}) is the resultant of two pressure drops. The first is the pressure drop caused by Darcy flow (P_D) while the second is the pressure drop caused by non-Darcy flow (P_{ND}) and the impact of skin factor in the vicinity of the wellbore (s_m). While Eq. (2) emphasizes the fact that the total pressure drop in (j^{th}) wellbore is the summation of the pressure drops inside this wellbore and its neighbors $\left(\sum_{j=1}^{j=N} P_{Dj}\, q_{Dj}\right)$ in addition to the impact of the non-Darcy flow and the mechanical skin factor of the (j^{th}) wellbore $\left(P_{NDj} + s_{mj}\right)q_{Dj}$.

The pressure summation term in Eq. (2) can be calculated using Laplace domain as follows:

$$\sum_{j=1}^{j=N} P_{Dj}\, q_{Dj} = \sum_{j=1}^{j=N} \mathcal{L}^{-1}\overline{P_{Dj}}\left(x_{wDj}, y_{wDj}, z_{wDj}, x_{Dj}, y_{Dj}, z_{Dj}, x_{eDj}, y_{eDj}, L_{Dj}, D_{Dj}\right)\overline{q_{Dj}} \quad (5)$$

To solve Eq. (5), the pressure drop caused by Darcy flow $(\overline{P_D})$, in the Laplace domain, should be calculated using four pressure terms [27-29]:

$$\overline{P_D} = \overline{P_{D1}} + \overline{P_{D2}} + \overline{P_{D3}} + \overline{P_{D4}} \quad (6)$$

where:

$$\overline{P_{D1}} = \frac{\pi}{s\sqrt{u}x_{eDj}}\left[e^{-\sqrt{u}|y_{Dj}-y_{wDj}|} + e^{-\sqrt{u}(2y_{eDj}-|y_{Dj}-y_{wDj}|)} + e^{-\sqrt{u}(y_{Dj}-y_{wDj})} + e^{-\sqrt{u}\left(2y_{eDj}-(y_{Dj}+y_{wDj})\right)}\right]\left[1 + \sum_{m=1}^{\infty} e^{-2m\sqrt{u}y_{eDj}}\right] \quad (7)$$

$$\overline{P_{D2}} = \frac{2}{s}\sum_{k=1}^{\infty}\frac{1}{k\sqrt{u+\left(\frac{k\pi}{x_{eDj}}\right)^2}}\sin\left(\frac{k\pi}{x_{eDj}}\right)\cos\left(k\pi\frac{x_{wDj}}{x_{eDj}}\right)\cos\left(k\pi\frac{x_{Dj}}{x_{eDj}}\right)\left[e^{-\sqrt{u+\left(\frac{k\pi}{x_{eDj}}\right)^2}|y_{Dj}-y_{wDj}|}+\right.$$
$$\left.e^{-\sqrt{u+\left(\frac{k\pi}{x_{eDj}}\right)^2}(2y_{eDj}-|y_{Dj}-y_{wDj}|)}+\quad e^{-\sqrt{u+\left(\frac{k\pi}{x_{eDj}}\right)^2}(y_{Dj}+y_{wDj})}+e^{-\sqrt{u+\left(\frac{k\pi}{x_{eDj}}\right)^2}(2y_{eDj}-(y_{Dj}+y_{wDj}))}\right]\left[1+\right.$$
$$\left.\sum_{m=1}^{\infty}e^{-2m\sqrt{u+\left(\frac{k\pi}{x_{eDj}}\right)^2}y_{eDj}}\right] \quad (8)$$

$$\overline{P_{D3}} = \frac{2\pi}{sx_{eDj}}\sum_{n=1}^{\infty}\frac{1}{\sqrt{u+(n\pi L_{Dj})^2}}\cos(n\pi z_{wDj})\cos(n\pi z_{Dj})\left[e^{-\sqrt{u+(n\pi L_{Dj})^2}|y_{Dj}-y_{wDj}|}+e^{-\sqrt{u+(n\pi L_{Dj})^2}(2y_{eDj}-|y_{Dj}-y_{wDj}|)}+\right.$$
$$\left.e^{-\sqrt{u+(n\pi L_{Dj})^2}(y_{Dj}+y_{wDj})}+e^{-\sqrt{u+(n\pi L_{Dj})^2}(2y_{eDj}-(y_{Dj}+y_{wDj}))}\right]\left[1+\sum_{m=1}^{\infty}e^{-2m\sqrt{u+(n\pi L_{Dj})^2}y_{eDj}}\right] \quad (9)$$

$$\overline{P_{D4}} = \frac{8}{s}\sum_{n=1}^{\infty}\cos(n\pi z_{wDj})\cos(n\pi z_{Dj})\sum_{k=1}^{\infty}\frac{1}{k\sqrt{u+(n\pi L_{Dj})^2+\left(\frac{k\pi}{x_{eDj}}\right)^2}}\sin\left(\frac{k\pi}{x_{eDj}}\right)\cos\left(k\pi\frac{x_{wDj}}{x_{eDj}}\right)\cos\left(k\pi\frac{x_{Dj}}{x_{eDj}}\right)$$
$$\left[e^{-\sqrt{u+(n\pi L_{Dj})^2+\left(\frac{k\pi}{x_{eDj}}\right)^2}|y_{Dj}-y_{wDj}|}+e^{-\sqrt{u+(n\pi L_{Dj})^2+\left(\frac{k\pi}{x_{eDj}}\right)^2}(2y_{eDj}-|y_{Dj}-y_{wDj}|)}+e^{-\sqrt{u+(n\pi L_{Dj})^2+\left(\frac{k\pi}{x_{eDj}}\right)^2}(y_{Dj}+y_{wDj})}+\right.$$
$$\left.e^{-\sqrt{u+(n\pi L_{Dj})^2+\left(\frac{k\pi}{x_{eDj}}\right)^2}(2y_{eDj}-(y_{Dj}+y_{wDj}))}\right]\left[1+\sum_{m=1}^{\infty}e^{-2m\sqrt{u+(n\pi L_{Dj})^2\left(\frac{k\pi}{x_{eDj}}\right)^2}y_{eDj}}\right]$$

(10)

while:

$$\overline{q_{Dj}} = \frac{q_j}{q_t} \quad (11)$$

where: (q_j) is the flow rate of (j^{th}) wellbore and (q_t) is the total flow rate of all wellbores.

the storativity-interporosity flow function (u) mentioned in Eqs. (7), (8), (9), and (10) is mathematically represented by:

$$u = sf(s) \quad (12)$$

where $[f(s) = 1.0]$ for homogenous single porous media.

The pressure drop caused by non-Darcy flow, mentioned in Eqs. (1), and (2), is considered mainly for gas reservoirs and a very minor part of oil reservoirs where the velocity of reservoir fluids could increase significantly to the limits of turbulent flow especially in the porous media close to the wellbores. It is given by:

$$P_{ND} = DQ_{sc} \quad (13)$$

and:

$$D = \delta\frac{\beta\gamma_g k_z}{L_w\mu r_w} \quad (14)$$

where: (δ) is a unit-conversion constant and (β) is known as the non-Darcy flow coefficient and mathematically formulated by a lot of models tabulated in the literature [30]. The non-Darcy pressure drop (P_{ND}) and mechanical skin factor in Eqs. (1), and (2) are calculated only for the wellbore where the pressure is calculated.

For a reservoir with a square drainage area, the pressure drops can be calculated from Eqs. (7), (8), (9), and (10) using $(x_{eD} = y_{eD})$. The wellbore spacing (D_{Dj}), mentioned in Eq. (5), for the rectangular and square drainage areas depleted by parallel wellbores is considered the difference between (y_{wDj}). It is calculated by:

$$D_{Dj} = y_{wDj} - y_{wD} \quad (15)$$

while the well spacing of radially distributed multilateral wellbores is represented by the deviation angle in the horizontal plane (θ). In Eq. (15), (y_{eD}) is the coordinate in the Y-direction of the wellbore where the pressure drop is calculated.

The impact of well spacing on the pressure response of rectangular reservoirs depleted by multiple horizontal wells, parallel or radial multilateral, is shown in Fig. (2a,b,c,d,e,f). Fig. (2a) represents the pressure behavior of three parallel wellbores of equal length ($L_D = 100.0$), distributed symmetrically with equal spacing among them, acting in different rectangular drainage areas ($A_D = 8.0, 16, and\ 32$). The following comments are inferred from Fig. (2a):

1- At early and intermediate production time, the pressure behavior and flow regimes, represented by the pressure derivative, are similar regardless of the drainage area. This fact indicates that the production pulse of each wellbore has not reached the adjacent wellbores i.e. the interference among these three wellbores has not occurred yet.

2- At late intermediate production time, the well spacing starts affecting the pressure behavior and flow regimes. This is physically can be felt by the change in the flow regimes that could be observed for the three reservoirs. For small drainage area ($A_D = 8.0$), and short well spacing ($D_D = 1.0$) there is an opportunity for developing "Early pseudo-steady state flow regime" that represents the impact of the no-flow boundaries among the three wellbores i.e. the mid-distance between two adjacent parallel wellbores. For big drainage area reservoirs ($A_D = 32$), and wide well spacing ($D_D = 4.0$), the expectations for developing "Intermediate radial flow regime" that represents the radial flow in the horizontal plane towards the wellbores that should be seen before early pseudo-steady state flow do not come true. Pseudo-radial flow or transition flow regime, the flow of reservoir fluids radially toward the wellbores in the horizontal plane, is observed before pseudo-steady state flow that represents the impact of the reservoir boundaries on the pressure behavior when the production pulse has reached these boundaries at late production time.

3- The interference among wellbores is observed earlier when the drainage area is small and the well spacing is short. Nevertheless, a long time might be elapsed before seeing the impact of well spacing and well interference when the drainage area is big.

4- For the same number of wellbores, the pressure drop decreases when the drainage area is big. Moreover, the starting time of pseudo-steady state flow of big drainage areas is longer than the one in the small drainage areas.

Fig. (2b) represents the pressure behavior and flow regimes of a rectangular reservoir, the drainage area is ($A_D = 32.0$), depleted by different parallel wellbores. The impact of well spacing is not seen during early and intermediate production time. However, a pseudo-radial flow regime is observed when the drainage area is depleted by a single wellbore ($N = 1.0$) as there is enough space for this flow regime to be developed. Transition flow is seen at late intermediate production time when two wellbores ($N = 2.0$) are used while early pseudo-steady state flow regime is developed when three wellbores ($N = 3.0$) are used. These two flow regimes, early pseudo-steady state and transition flow regime, represent the impact of well spacing and interference. For the same drainage area, the pressure drop increases with the increase of wellbores and the starting time of pseudo-steady state flow decrease when more wellbores are used.

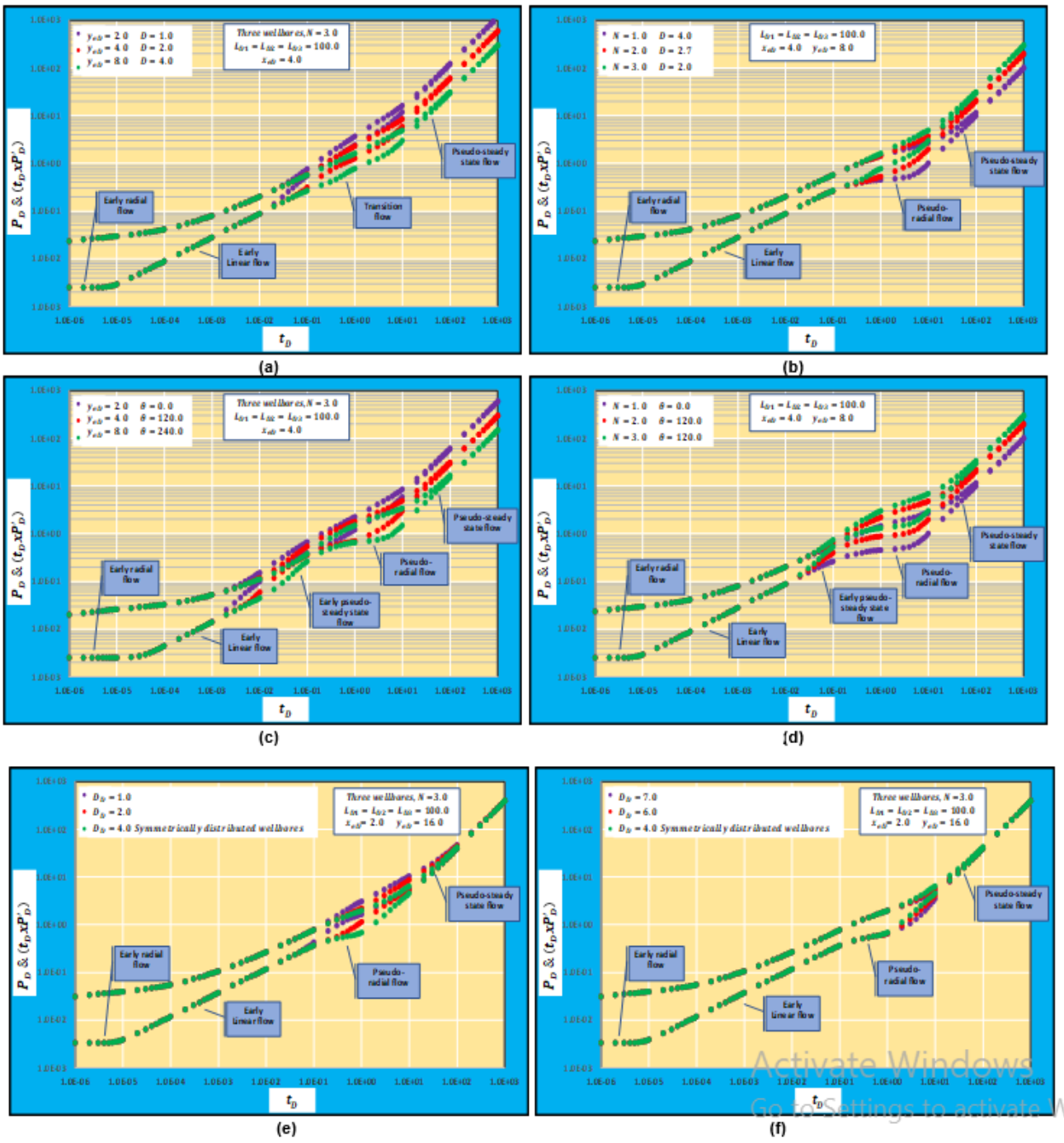

Figure 2: Pressure and pressure derivative behaviors of rectangular reservoirs (a) Three parallel wellbores and different drainage areas (b) Different parallel wellbores and constant drainage area (c) Three radial multilateral wellbores and different drainage areas (d) Different radial multilateral wellbores and constant drainage area (e) Three parallel wellbores unsymmetrically distributed close to mid-wellbore (f) Three parallel wellbores unsymmetrically distributed close to reservoir boundary.

Fig. (2c) represents the pressure and pressure derivative of three radially distributed multilateral wellbores acting in rectangular reservoirs of different drainage areas while Fig. (2d) depicts the pressure and pressure derivative of different multilateral wellbores acting in the same rectangular drainage area. The following comments are inferred from Fig. (2c, d):

1- The impact of well spacing and interference for radially distributed multilateral wellbores is observed earlier than the impact seen for parallel wellbores for the same drainage area and the number of wellbores. This is

physically explained by the short spacing between wellbores close to the heel of these wellbores. Similar to the parallel wellbores, decreasing the drainage area facilitates the well interference.

2- Early pseudo-steady state and pseudo-radial flow regimes are observed more clear than parallel wellbores. They are very well developed when big drainage areas are depleted by multilateral wellbores.

3- Because the impact of well spacing and interference is seen at early intermediate production time, an early linear flow regime that represents the flow of reservoir fluids linearly towards the wellbore may not last for a long time especially if the drainage area is small.

If the wellbores are symmetrically distributed in the drainage areas, pseudo-steady state flow, developed at late production time, is reached faster for small drainage areas than large drainage areas. This is, in fact, because of the drainage area itself but not the impact of well spacing. However, pseudo-steady state flow of symmetrically distributed wellbores may need a longer time to be observed than unsymmetrically distributed wellbores when the well spacing among wellbores is narrow as it can be seen in Fig. (2e). Fig. (2e) represents the pressure behavior and flow regimes of three parallel wellbores acting in the same drainage area (A_D=32.0) with different well spacing between wellbores. The three wellbores, in this case, are symmetrically and unsymmetrically distributed close to the mid-point of the reservoir boundary (y_eD). Symmetrically distributed wellbores with equal distance between them, (D_D=4.0), in Fig. (2e) means that the distance to the reservoir boundary is shorter than the distance between wellbores and reservoir boundary for the cases of (D_D=1.0,and 2.0). Because of that, the production pulse could reach the boundary faster for the case of (D_D=4.0) than the cases of (D_D=1.0,and 2.0). However, when the wellbores are unsymmetrically distributed close to the reservoir boundary as it can be seen in Fig. (2f), pseudo-steady state flow is reached faster than the unsymmetrical distribution of wellbores close to the reservoir mid-point because of the shorter distance to the reservoir boundary for the first case than the second.

The impact of well spacing on the production rate and cumulative production behaviors is shown in Fig. (3a,b,c,d). Fig. (3a), tells us that the production rate and cumulative production at intermediate and late production time increase with increasing the number of the parallel wellbores and thereby narrowing the spacing among them. It shows also no changes neither in the production rate nor cumulative production behavior at early and early intermediate production time. While the impact of well spacing is seen at late production time on the production rate and cumulative production behavior when different numbers of parallel wellbores are used for depleting the same drainage area as it is depicted in Fig. (3b).

The same comments are obtained for the two cases of radially distributed multilateral wellbores as it is shown in Fig. (3c) for three wellbore and different drainage areas and Fig. (3d) for different numbers of wellbores acting in the same drainage area. As a general statement, production rate and cumulative production increase as the drainage area increases for both parallel and radial wellbores. However, they decrease when the number of the wellbores increases in the same drainage area because of the interferences between wellbores. Furthermore, the impact of the drainage area on the production and cumulative production of parallel and radial wellbores is more observable than the impact of the number of wellbores. Increasing the number of the wellbore may not change significantly the production rate and cumulative production i.e. when three wellbores are used, the decrease is not significant compared to two wellbores.

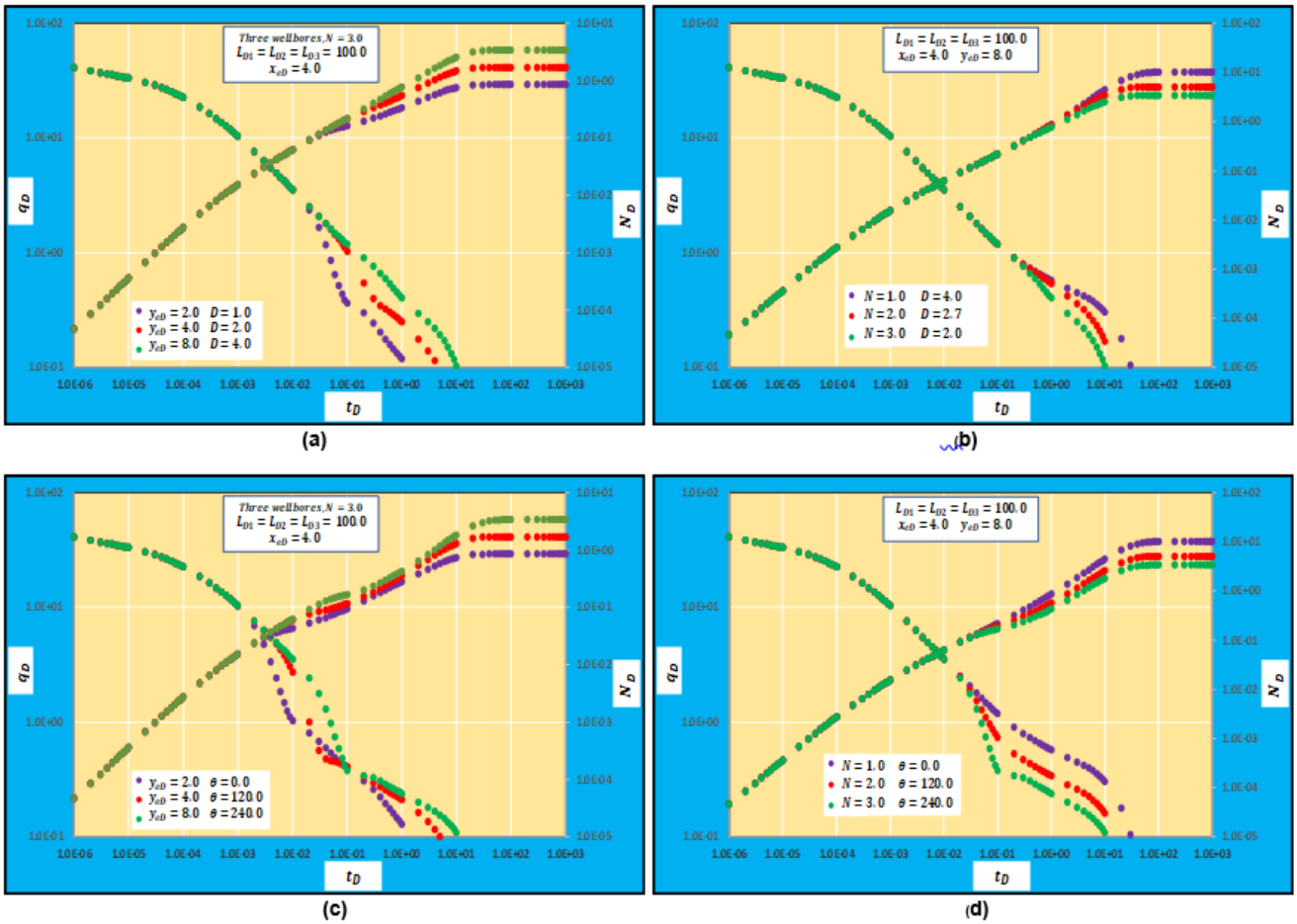

Figure 3: Production and cumulative production behaviors of rectangular reservoirs (a) Three parallel wellbores and different drainage areas (b) Different parallel wellbores and constant drainage area (c) Three radial multilateral wellbores and different drainage areas (d) Different radial multilateral wellbores and constant.

For a circular drainage area of a radius (r_e) and depleted by radially distributed multiple horizontal wells, as shown in Fig. (4), different models are required to calculate the pressure drops. The general solution of the pressure drop in dimensionless form, in this case, consists of three pressure terms [29].

$$\overline{P_{D1}} = \frac{1}{2s}\int_{-1}^{1}\left[K_o\left(r_D\sqrt{u}\right) + \frac{I_o(r_D\sqrt{u})K_1(r_{eDj}\sqrt{u})}{I_1(r_{eDj}\sqrt{u})}\right]dr_D \tag{16}$$

$$\overline{P_{D2}} = \frac{1}{s}\sum_{n=1}^{\infty} cos\left(n\pi z_{Dj}\right)cos\left(n\pi z_{wDj}\right)\int_{-1}^{1}\left[K_o\left(r_D\sqrt{u+\left(n\pi L_{Dj}\right)^2}\right)\right]dr_D$$

(17)

$$\overline{P_{D3}} = \frac{1}{s}\sum_{n=1}^{\infty} cos\left(n\pi z_{Dj}\right)cos\left(n\pi z_{wDj}\right) + \int_{-1}^{1}\left[\frac{I_o\left(r_D\sqrt{u+\left(n\pi L_{Dj}\right)^2}\right)K_1\left(r_{eDj}\sqrt{u+\left(n\pi L_{Dj}\right)^2}\right)}{I_1\left(r_{eDj}\sqrt{u+\left(n\pi L_{Dj}\right)^2}\right)}\right]dr_D \tag{18}$$

The wellbore spacing of the circular drainage area is considered as the deviation angle (θ) between the wellbore where the pressure is calculated and other wellbores. Mathematically, the wellbore length is represented by:

$$L_{Dj} = \frac{L_{wj}}{h}\sqrt{\frac{k_z}{k}}cos\left(\theta_j\right) \tag{19}$$

where $\left(k = \sqrt[3]{k_x k_y k_z}\right)$ is the reservoir permeability.

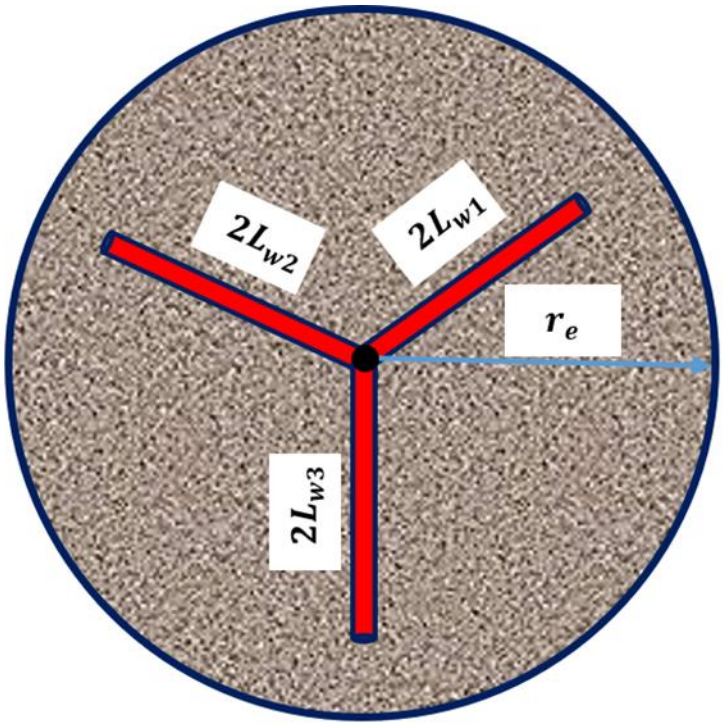

Figure 4: Circular bounded reservoir with radially distributed multiple horizontal wells.

The pressure and pressure derivative behaviors of reservoirs with circular drainage areas depleted by different wellbores and different well spacings are shown in Fig. (5a,b). Similar to rectangular reservoirs behavior depleted by parallel and radial multilaterals, the impact of well spacing is observed at intermediate and late production time when the circular drainage areas of different sizes ($r_{eD} = 2.0, 4.0, and\ 8.0$) are depleted by three wellbores of equal length ($L_D = 100.0$) as shown in Fig. (5a). The conclusion that could be drawn here is the possibility to see the impact of well spacing and interference very early, probably after the early radial flow regime, when the drainage area is small and multiple wellbores are used. The impact of well spacing is seen at early and intermediate production time when different numbers of wellbores are used to deplete a circular drainage area of ($A_D = 16.0\pi$) as shown in Fig. (5b). The transition flow regime represents the effect of the interference among wellbores that could be occurred at early and intermediate production time especially close to the mid-point where the horizontal wellbores join the vertical wellbore. It is developed and observed after early linear or early pseudo-steady state flow regime and before reaching pseudo-steady state flow regime as the production pulse along each wellbore length could impact the production pulse of the adjacent wellbores. This flow regime may have a constant pressure derivative behavior, similar to the pseudo-radial flow regime, but it is not equal to (0.5). The value of the pressure derivative of the transition flow regime, in dimensionless form, is mathematically represented by:

$$(t_D x P'_D)_{TF} = N(t_D x P'_D)_{RF} = 0.5N \quad (20)$$

where: $(t_D x P'_D)_{TF}$ is the pressure derivative of the transition flow regime and $(t_D x P'_D)_{RF}$ is the pseudo-radial flow regime pressure derivative that is equal to (0.5) while (N) is the number of wellbores.

The production rate and cumulative production behavior of a circular drainage area is similar also to the rectangular reservoirs. Increasing the number of the wellbores acting in the same drainage area or increasing the well spacing between wellbores used to deplete the same reservoirs causes an increase in the production rate and cumulative production as it can be seen in Fig. (6a,b).

For all cases, rectangular and circular drainage areas, the pressure derivative of the early linear flow regime is the same and equals, in dimensionless form, to:

$$(t_D x P'_D)_{LF} = \frac{1}{4L_D} \quad (21)$$

where: $(t_D x P'_D)_{LF}$ is the pressure derivative of the early radial flow regime and (L_D) is the length of wellbores. It is important to emphasize that the early pressure derivative demonstrates the same value of a single wellbore of a specific length even though multiple wellbores are used. Physically, this is true as the early radial flow regime is

developed at early production time around the wellbore where the pressure drop is calculated. Accordingly, it is not affected by the wellbore spacing.

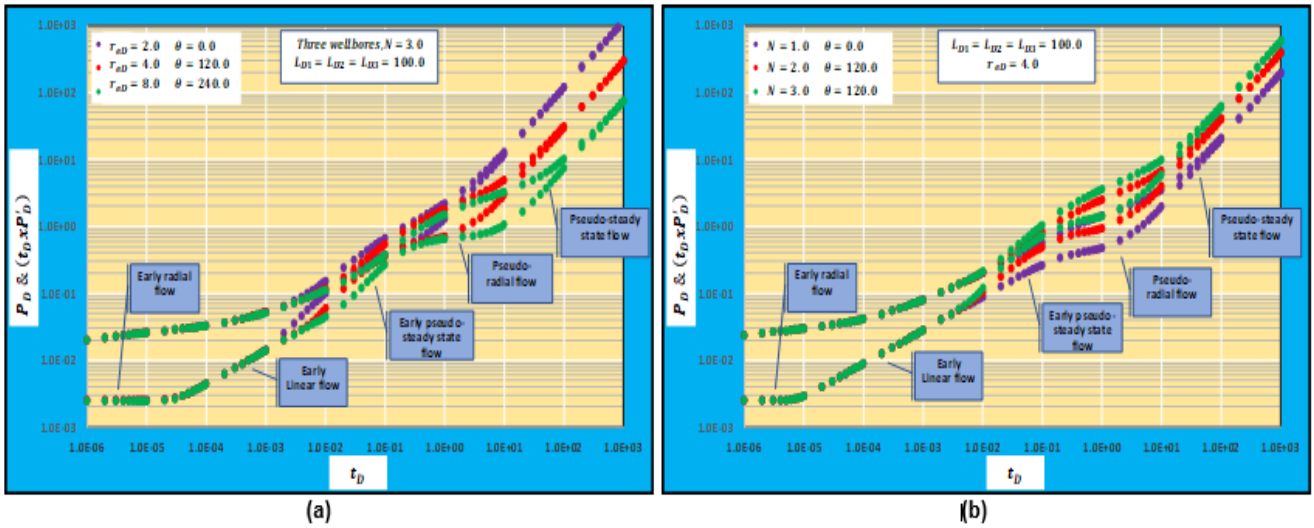

Figure 5: Pressure and pressure derivative behaviors of circular drainage area (a) Three wellbores and different drainage areas (b) Different wellbores and constant drainage area.

The comparison between the case where the wellbore length and flow rate are the same and the case where different wellbore lengths and flow rates are used is shown in Fig. (7a,b). Fig. (7a) shows the difference between the two cases for rectangular reservoirs while Fig. (7b) for circular reservoirs. For both cases, only intermediate production flow regimes i.e. early pseudo-steady state and transition flow regimes are impacted very slightly by the change in wellbore length and flow rate. The impact on the pseudo-steady state is not significant. The reason for that belongs to the fact the total pressure drop is mainly contributed by the pressure drop of the wellbore where the pressure drop is calculated. Very minor contributions are given by the other wellbores to the total pressure drops depending on the well spacing. Therefore, the change in the wellbore lengths and flow rates of the neighbor wells may not change the pressure drop significantly unless the well spacing is very short.

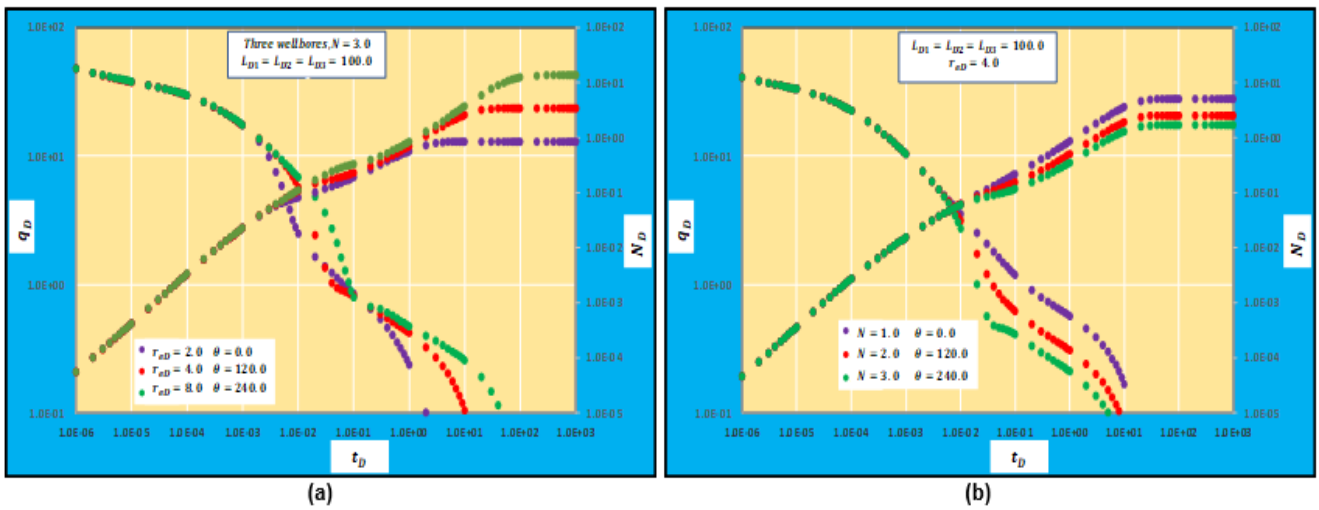

Figure 6: Production and cumulative production behaviors of circular drainage area (a) Three wellbores and different drainage areas (b) Different wellbores and constant drainage area.

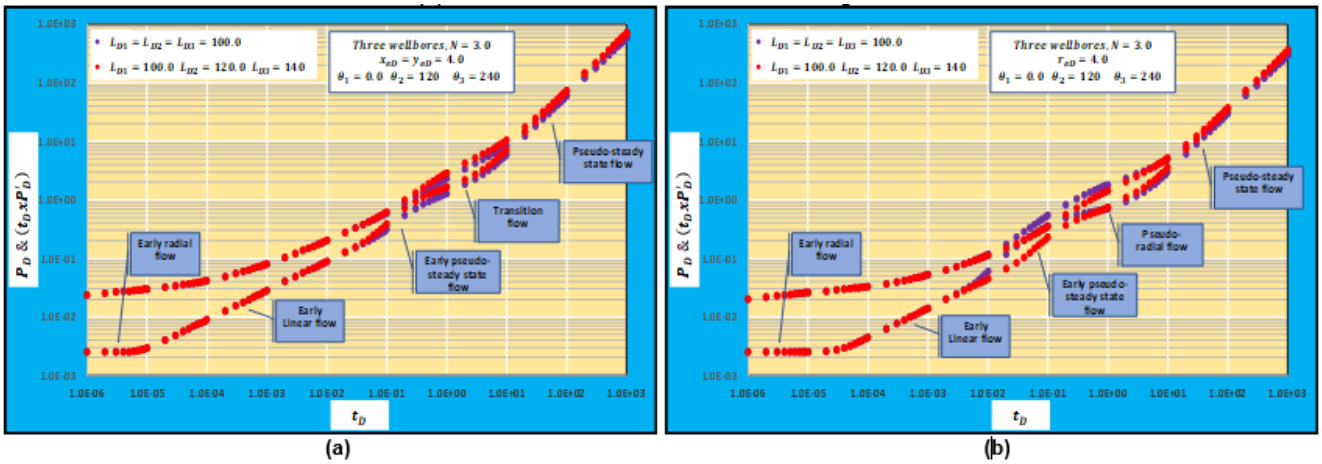

Figure 7: Pressure and pressure derivative behavior of (a) Rectangular reservoirs (b) Circular reservoirs.

3. Pressure drops' models of pseudo-steady state flow

Pseudo-steady state condition is observed when the production pulse has reached the reservoir boundary. It is seen always observed after a long production time. Accordingly, the long-time approximation is required to develop the pressure drop' models for this condition. Therefore, the storativity-interporosity flow function (u) mentioned in Eq. (12) is replaced by (s) as the limit of the function $[f(s)]$ reaches (1.0) when $(s \to 0.0)$. At long production time, the value of (s) is small enough to consider the terms $\sqrt{u+(k\pi/x_{eDj})^2}$, $\sqrt{u+(n\pi L_{Dj})^2}$, and $\sqrt{u+(n\pi L_{Dj})^2+(k\pi/x_{eDj})^2}$ in Eqs. (8), (9), (10), (17), and (18) as $(k\pi/x_{eDj})$, $(n\pi L_{Dj})$, and $\sqrt{(n\pi L_{Dj})^2+(k\pi/x_{eDj})^2}$ respectively. Considering the abovementioned approximations, the mathematical models of the pressure drop during pseudo-steady state conditions for multiple horizontal wells acting in rectangular reservoirs can be obtained from Eqs. (7), (8), (9), and (10):

$$P_{D1} = 2\pi t_{DA} + 2\pi \frac{y_{eDj}}{x_{eDj}}\left(\frac{1}{3} - \frac{y_{Dj}}{y_{eDj}} + \frac{y_{Dj}^2+y_{wDj}^2}{2y_{eDj}}\right) \tag{22}$$

$$P_{D2} = \frac{2x_{eDj}}{\pi}\sum_{k=1}^{\infty}\frac{1}{k^2} sin\left(\frac{k\pi}{x_{eDj}}\right) cos\left(k\pi\frac{x_{wDj}}{x_{eDj}}\right) cos\left(k\pi\frac{x_{Dj}}{x_{eDj}}\right)\left[e^{-k\pi|y_{Dj}-y_{wDj}|} + e^{-k\pi\left(2\frac{y_{eDj}}{x_{eDj}}-|y_{Dj}-y_{wDj}|\right)} + e^{-k\pi(y_{Dj}-y_{wDj})} + e^{-k\pi\left(2\frac{y_{eDj}}{x_{eDj}}-(y_{Dj}-y_{wDj})\right)}\right]\left[1+\sum_{m=1}^{\infty}e^{-2mk\pi\frac{y_{eDj}}{x_{eDj}}}\right] \tag{23}$$

$$P_{D3} = \frac{2}{x_{eDj}L_{Dj}}\sum_{n=1}^{\infty}\frac{1}{n} cos(n\pi z_{Dj}) cos(n\pi z_{wDj})\left[e^{-n\pi L_{Dj}|y_{Dj}-y_{wDj}|} + e^{-n\pi L_{Dj}(2y_{eDj}-|y_{Dj}-y_{wDj}|)} + e^{-n\pi L_{Dj}(y_{Dj}-y_{wDj})} + e^{-n\pi L_{Dj}\left(2y_{eDj}-(y_{Dj}-y_{wDj})\right)}\right]\left[1+\sum_{m=1}^{\infty}e^{-2mn\pi L_{Dj}y_{eDj}}\right] \tag{24}$$

$$P_{D4} = 4\sum_{n=1}^{\infty} cos(n\pi z_{Dj}) cos(n\pi z_{wDj}) \sum_{k=1}^{\infty}\frac{1}{k\sqrt{(n\pi L_{Dj})^2+(k\pi/x_{eDj})^2}} sin\left(\frac{k\pi}{x_{eDj}}\right) cos\left(k\pi\frac{x_{wDj}}{x_{eDj}}\right) cos\left(k\pi\frac{x_{Dj}}{x_{eDj}}\right)$$

$$\left[e^{-\sqrt{(n\pi L_{Dj})^2+(k\pi/x_{eD})^2}|y_{Dj}-y_{wDj}|} + e^{-\sqrt{(n\pi L_{Dj})^2+(k\pi/x_{eDj})^2}(2y_{eDj}-|y_{Dj}-y_{wDj}|)} + e^{-\sqrt{(n\pi L_{Dj})^2+(k\pi/x_{eDj})^2}(y_{Dj}-y_{wDj})} + e^{-\sqrt{(n\pi L_{Dj})^2+(k\pi/x_{eDj})^2}\left(2y_{eDj}-(y_{Dj}-y_{wDj})\right)}\right]\left[1+\sum_{m=1}^{\infty}e^{-2m\sqrt{(n\pi L_{Dj})^2+(k\pi/x_{eDj})^2}y_{eDj}}\right] \tag{25}$$

Needless to say, that Eqs. (22), (23), (24), and (25) can be used for square drainage areas with $(x_{eD} = y_{eD})$. While the long-time approximation of the pressure drops of circular drainage areas during pseudo-steady state conditions can be obtained from Eqs. 916), (17), and (18):

$$P_{D1} = 2\pi t_{DA} + ln(r_{eDj}) + 0.25 \quad (26)$$

$$P_{D2} = 0.25\left[(x_{Dj}-1)ln\left\{(x_{Dj}-1)^2 + y_{Dj}^2\right\} - (x_{Dj}+1)ln\left\{(x_{Dj}+1)^2 + y_{Dj}^2\right\} - 2y_{Dj}arctan\left(\frac{2y_{Dj}}{x_{Dj}^2+y_{Dj}^2-1}\right)\right]$$

(27)

$$P_{D3} = \frac{y_{Dj}^2}{r_{eDj}^2} + \frac{(x_{Dj}+1)^3-(x-1)^3}{12r_{eDj}^2} \quad (28)$$

$$P_{D4} = \sum_{n=1}^{\infty} cos(n\pi z_{Dj})cos(n\pi z_{wDj}) \int_{-1}^{1} K_o(n\pi L_{Dj}\bar{r}_D)da \quad (29)$$

$$P_{D5} = \sum_{n=1}^{\infty} cos(n\pi z_{Dj})cos(n\pi z_{wDj}) + \int_{-1}^{1} \frac{I_o(n\pi L_{Dj}\bar{r}_D)K_1(n\pi L_{Dj}r_{eDj})}{I_1(n\pi L_{Dj}r_{eDj})}da \quad (30)$$

where:

$$a = \sqrt{(x_{Dj}-1)^2 + {y_{Dj}}^2} \quad (31)$$

The pressure distribution and pressure derivative profile during pseudo-steady state flow conditions for rectangular reservoirs depleted by parallel and radial wellbores are given in Fig. (8a,b). While Fig. (9a,b) shows these behaviors for circular drainage areas. Similar to the conclusions that have been reached in Section-2, the well spacing have a significant impact on the pressure behavior during pseudo-steady state flow conditions regardless of the reservoir size and the number of the wellbores and their distribution. The impact of well spacing and interference on the pressure behavior during pseudo-steady state flow at late production time is bigger than the impact during intermediate production time i.e. late linear flow, early pseudo-steady state flow, and transition flow regime. This fact could be explained by the dual influence of the reservoir boundaries and the well spacing when the production pulse has reached these boundaries.

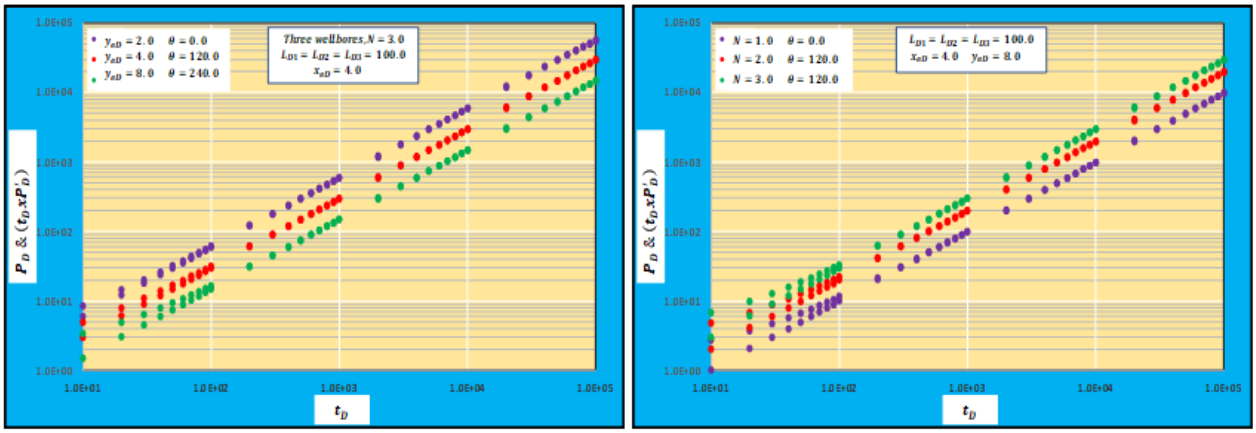

(a) (b)

Figure 8: Pseudo-steady state pressure and pressure derivative behaviors of rectangular drainage areas (a) Three radial multilaterals wellbores and different drainage areas (b) Different radial multilaterals wellbores and constant drainage areas.

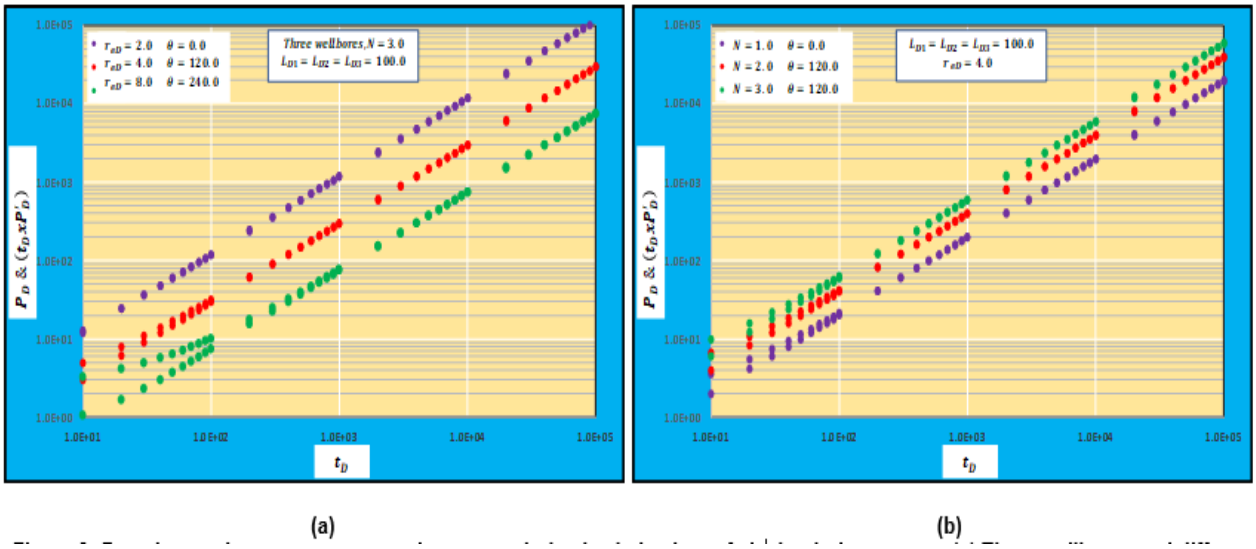

Figure 9: Pseudo-steady state pressure and pressure derivative behaviors of cicular drainage areas (a) Three wellbores and different drainage areas (b) Different wellbores and constant drainage areas.

4. Productivity index

The productivity index of a single horizontal wellbore acting in a finite reservoir may have two patterns. The first is during transient state flow at early and intermediate production time when the pressure could change sharply with time for the case of constant sandface flow rate or when the flow rate could change sharply with time for the case of constant bottom hole flowing pressure. It is calculated for the two cases respectively by:

$$J_D|_{constant\ q} = \frac{1}{P_{wD}} \tag{32}$$

$$J_D|_{constant\ P_{wf}} = \frac{1}{(1/q_D)} \tag{33}$$

The second occurs during pseudo-steady state flow conditions when the production pulse has reached the reservoir boundary. The productivity index, in this case, is characterized by a stabilized value that can be calculated for the constant sand face flow rate and constant bottom hole flowing pressure respectively by:

$$J_D|_{constant\ q} = \frac{1}{P_{wD} - 2\pi t_{DA}} \tag{34}$$

$$J_D|_{constant\ P_{wf}} = \frac{1}{(1/q_D) - 2\pi N_D/q_D} \tag{35}$$

The same patterns could be observed when the reservoirs are depleted by multiple horizontal wellbores. For transient state flow condition of multiple horizontal wellbores acting in different shape reservoirs, the productivity index of constant sand face flow rate can be calculated by [31]:

$$\left[J_D|_{constant\ q}\right] = [([A] + [B])^{-1}\ ]\overrightarrow{q_D} \tag{36}$$

where:

$$(A) = \begin{bmatrix} P_{D11} & P_{D12} & P_{D13} & \ldots\ldots & P_{D1N} \\ P_{D21} & P_{D22} & P_{D23} & \ldots\ldots & P_{D2N} \\ \ldots & \ldots & \ldots & \ldots\ldots & \ldots \\ P_{DN1} & P_{DN2} & P_{DN3} & \ldots\ldots & P_{DNN} \end{bmatrix} \tag{37}$$

$$(B) = \begin{bmatrix} (P_{ND1} + s_{m1}) \\ (P_{ND2} + s_{m2}) \\ \ldots\ldots \\ (P_{NDN} + s_{mN}) \end{bmatrix} \tag{38}$$

$$\overrightarrow{q_D} = \begin{bmatrix} q_{D1} \\ q_{D2} \\ \dots \\ q_{DN} \end{bmatrix} \quad (39)$$

where the pressure terms in Eq. (37) are calculated by Eq. (6) and flow rate terms in Eq. (39) are calculated by Eq. (11). While for pseudo-steady state flow conditions, the pressure terms in Eq. (37) are subtracted by $(2\pi t_{DA})$. It is important to emphasize that Eq. (6) is calculated for the transient state flow conditions using Eqs. (7), (8), (9), and (10) for rectangular reservoirs and Eqs. (16), (17), and (18) for circular drainage areas. While Eq. (6) is calculated for the pseudo-steady state flow conditions using Eqs. (22), (23), (24), and (25) for rectangular reservoirs and Eqs. (26), (27), (28), (29), and (30) for circular drainage areas.

The productivity index of constant bottom hole flowing pressure of multiple horizontal wellbores can be calculated using the same concepts of constant sand face flow rate. Mathematically, it is represented by:

$$\left[J_D|_{constant\ P_{wf}}\right] = [\ A\ ]^{-1}[\overrightarrow{q_D}] \quad (40)$$

where:

$$(A) = \begin{bmatrix} 1/q_{D11} & 1/q_{D12} & 1/q_{D13} & \dots\dots & 1/q_{D1N} \\ 1/q_{D21} & 1/q_{D22} & 1/q_{D23} & \dots\dots & 1/q_{D2N} \\ \dots & \dots & \dots & \dots\dots & \dots \\ 1/q_{DN1} & 1/q_{DN2} & 1/q_{DN3} & \dots\dots & 1/q_{DNN} \end{bmatrix} \quad (41)$$

$$\overrightarrow{q_D} = \begin{bmatrix} q_{D1} \\ q_{D2} \\ \dots \\ q_{DN} \end{bmatrix} \quad (42)$$

where the flow rate terms in Eq. (41) are calculated by Eq. (3) while the flow rate terms in Eq. (42) are calculated by Eq. (11). The real-time productivity index can be calculated from the dimensionless productivity index, calculated by Eqs. (32), (33), (34), (35), (36), and (40) using:

$$J = CJ_D \quad (43)$$

where:

$$C = \frac{kh}{141.2\mu B_o} \quad \text{for oil reservoirs} \quad (44)$$

$$C = \frac{kh}{1422T} \quad \text{for gas reservoirs using a pseudo-pressure function} \quad (45)$$

The transient and stabilized pseudo-steady state productivity index of the rectangular reservoirs is shown in Fig. (10a,b,c,d) for constant sand face flow rate (J_{Dq}), and constant bottom hole flowing pressure (J_{DP}) while Fig. (11a,b) gives the productivity index of circular drainage areas. For better understanding the productivity index behavior with the production time, the following three flow periods will be considered:

4-1-Eealy production time

The productivity index does not change at early production time during transient state flow when early radial and early linear flow regimes dominate the flow in the porous media regardless of the drainage area shape and size and the number of the wellbores. Mathematically, this is true as the productivity index is calculated based on the flow rate obtained from one of the wellbores and the corresponding pressure drop. The flow rate is assumed constant and the pressure drop at the wellbore of interest does not change even though the production from the neighbor wells unless the well spacing is very narrow i.e. the impact of the production from other wellbores has not reached the wellbore where the pressure is calculated. In other words, there is no impact for the well spacing on the trainset productivity index at early production time. Physically, the reason beyond this behavior is the "infinite acting behavior" of each drainage area assigned to each wellbore.

4-2-Intermediate production time

Intermediate production time is characterized by the dominance of the linear flow regime in the porous media when the wellbores do not undergo the interference if the well spacing is wide enough. Therefore, the productivity index, in this case, is constant for all reservoir shapes and sizes and the wellbore number and distribution. However, if the well spacing is not wide enough, the well interference starts affecting the pressure drop and the productivity

index accordingly starts to be impacted by the drainage area size and shape and the number of the wellbores. At this time, the infinite acting behavior is no longer existed and the finite acting behavior becomes the dominant and determined by the drainage area allocated to each wellbore. Therefore, the linear flow regime vanishes and the early pseudo-steady state is developed followed by the transient flow regime. The productivity index during these two flow regimes shows different behaviors. It increases significantly when the drainage area, depleted by the same number of wellbores, becomes bigger while it decreases when the same drainage area is depleted by increasing the number of wellbores. The abovementioned behaviors of the productivity index are seen for parallel and radial wellbores in circular and rectangular reservoirs. The most interesting point here is the possibility of reaching a stabilized productivity index when the early pseudo-steady state flow regime is developed. The index for this flow regime is greater than the stabilized productivity index obtained during pseudo-steady state flow typically observed at late production time.

4-3-Late production time

Pseudo-steady state flow regime is typically observed at late production time when the production pulse reaches reservoir boundaries. The productivity index behavior shows "stabilized constant value" during pseudo-steady state flow. This stabilized value is affected by the number of the wellbores and the well spacing. For three wellbores acting in different drainage areas, the stabilized productivity index increases significantly with the increase of well spacing represented by the increase of the drainage area while it decreases with the increase of the wellbore numbers acting in the same drainage area as the well spacing becomes narrow when a big number of wellbores are used.

Figs. (10a,b,c,d), and (11a,b) also confirm the following facts regarding the transient and stabilized pseudo-steady state productivity index:

1- The index slightly decreases with the production time at early production when reservoir fluids flow radially toward wellbores in the vertical plane. However, the index sharply declines with the production time at intermediate production when reservoir fluids flow linearly toward wellbores in the horizontal plane.
2- The index of parallelly distributed wellbores in rectangular reservoirs is less than the index of the same number of multilateral wellbores radially distributed in the same drainage area. While the index of radially distributed wellbores in circular drainage areas is better than the index of rectangular reservoirs.
3- The index reaches the stabilized value at late production time when pseudo-steady state flow condition is reached. The starting time of pseudo-steady state flow depends on the reservoir size and the number of the wellbores and their distribution in the porous media. However, the index tends to reach this stabilized value even before reaching pseudo-steady state flow conditions. This could be explained by developing the early pseudo-steady state flow regime where the no-flow boundaries between two adjacent wellbores impact the pressure and act as the physical reservoir boundaries.
4- The index of a constant sand face flow rate approach is slightly more than the index of a constant bottom hole flowing pressure approach.

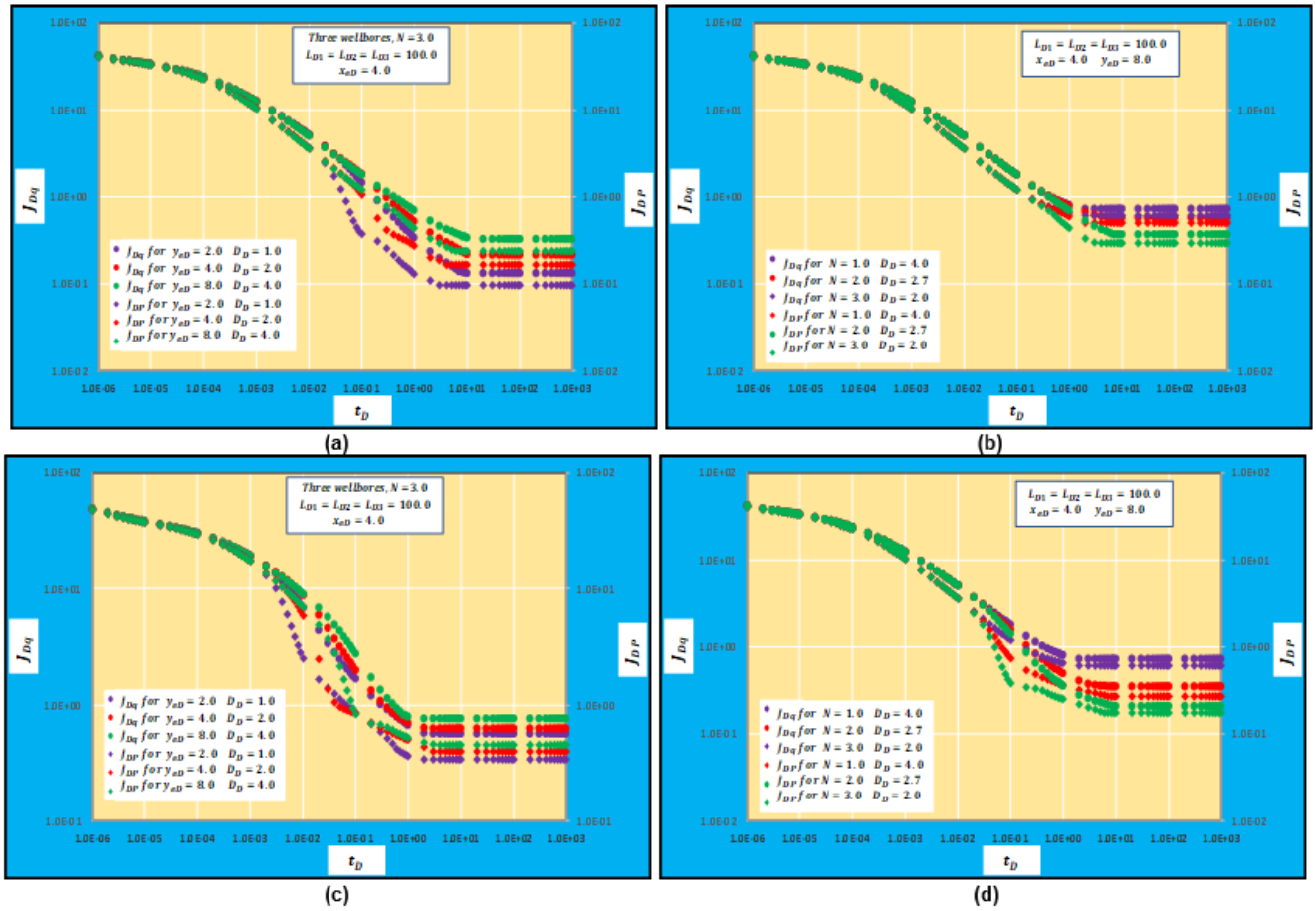

Figure 10: Transient and pseudo-steady state productivity index of rectangular drainage areas (a) Three parallel wellbores and different drainage areas (b) Different parallel wellbores and constant drainage areas (c) Three radial multilaterals and different drainage areas (b) Different radial multilaterals and constant drainage areas.

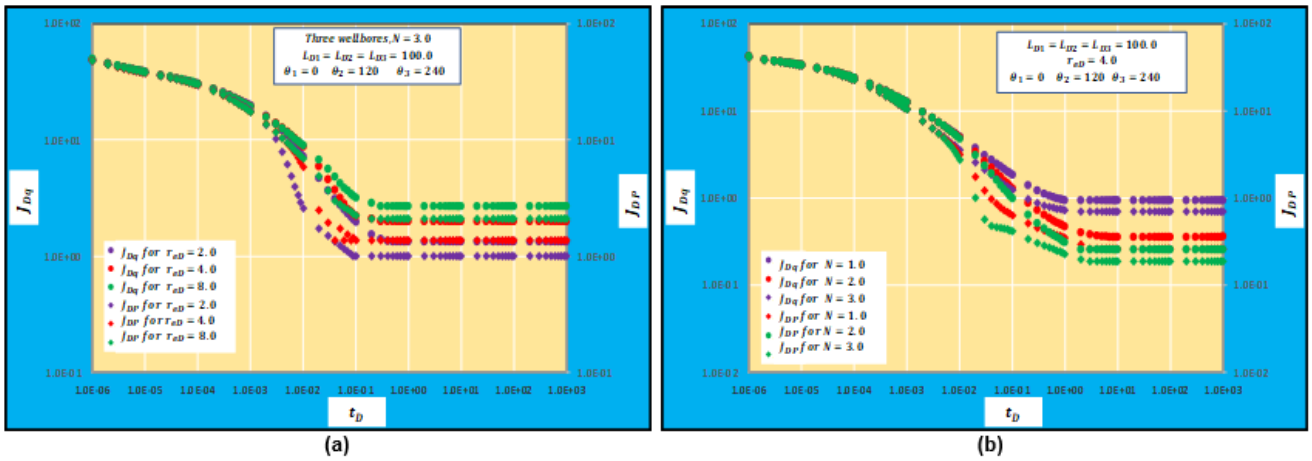

Figure 11: Transient and pseudo-steady state productivity index of circular drainage areas (a) Three wellbores and different drainage areas (b) Different wellbores and constant drainage areas.

5. Limitations

The limitations of the study presented in this paper are summarized by the following points:

1-The assumptions used in formulating the pressure and pseudo-pressure, flow rate and cumulative production, and productivity index models. These assumptions are:

- The flow is considered single phase only i.e. oil or gas.
- The pressure drop caused by the flow inside wellbores is not included.
- The wellbores are assumed horizontally extending in the porous media i.e. the azimuth angle is zero. They are symmetrically distributed in the vertical plane i.e. $(z_{wD} = 0.5)$.
- The reservoirs are assumed homogenous and isotropic in this study with uniform thickness. Dual porosity and permeability reservoirs are not included in this study.
- The physical properties of reservoir fluid are constant.
- Even though the non-Darcy pressure drop is mentioned during the formulation of the models, it is not considered in this study i.e. $(P_{ND} = DQ_{sc} = 0.0)$.

2- The initial reservoir condition is given by:

$$P_D(x_D, y_D, t_D = 0.0) = 0.0 \quad (46)$$

while reservoir boundary conditions are:

$$\frac{\partial P_D}{\partial x_D} = 0.0 \quad at \ x_D = x_{eD} \quad (47)$$

$$\frac{\partial P_D}{\partial y_D} = 0.0 \quad at \ y_D = y_{eD} \quad (48)$$

$$\frac{\partial P_D}{\partial r_D} = 0.0 \quad at \ r_D = r_{eD} \quad (49)$$

$$\frac{\partial P_D}{\partial z_D} = 0.0 \quad at \ z_D = 0.0 \quad and \ z_D = 1.0 \quad (50)$$

and inner wellbore condition is:

$$P_D(x_{wD}, y_{wD}, t_D) = P_{wD} \quad (51)$$

3- Circular, rectangular, and square drainage areas are considered in this study.

Appendix-A gives the mathematical definitions of all dimensionless parameters used in the abovementioned sections.

6. Application

A verification process of the proposed approach in this study for predicting pressure and pressure derivative, flow rate and cumulative production, and productivity index of multiple horizontal wellbores acting in bounded rectangular reservoirs is introduced in this section. The verification is conducted by the comparison of the results obtained from the analytical models presented in this paper using one of the state-of-the-art computational tools [32] and the industrial simulation software [33]. The data set used in the verification process is given in Table-1 while the reservoir configuration and the wellbore distribution are shown in Fig. (12). It is assumed that the reservoir is homogenous and isotropic with a single-phase oil flow only. The wellbores are parallelly distrusted in the porous media. The following steps are followed during the verification:

Table-1: Data set used in the verification process.

Reservoir length, x_e	6000.0 ft
Reservoir width, y_e	9000.0 ft
Number of wellbores, N	3.0
Length of wellbore, $2L_w$	3000.0 ft
Reservoir thickness, h	50.0 ft
Reservoir permeability, $k_v = k_H$	20.0 md
Reservoir porosity, $\emptyset$	0.15
Reservoir compressibility, c_t	$1.5*10^{-5}$ psi^{-1}
Well spacing	2250.0 ft
Reservoir fluid viscosity, μ	0.8 cp

Reservoir temperature, T	200 °F
Wellbore radius, r_w	0.5 ft
Oil formation volume factor	1.15 rbbl/Stb
Reservoir pressure	5000 psi

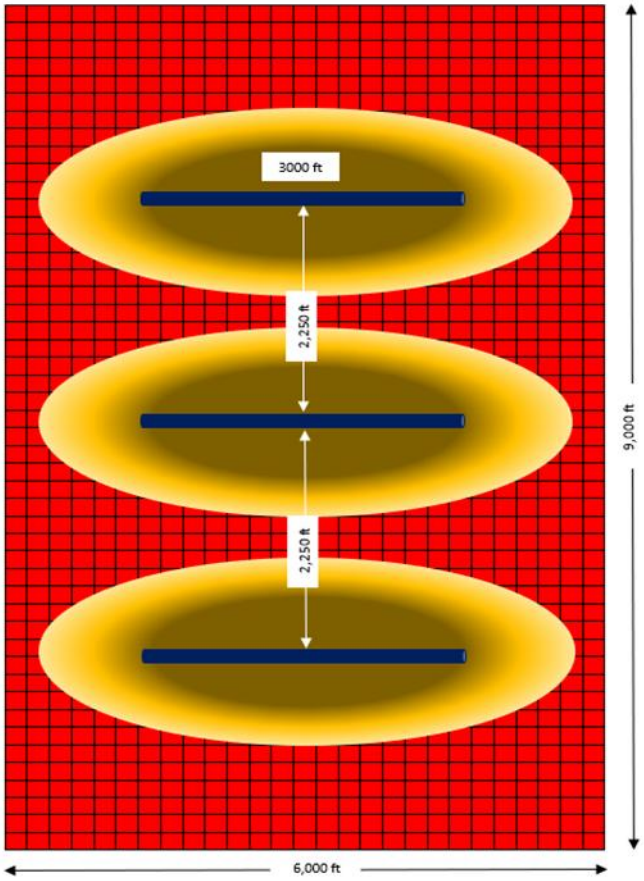

Figure 12: Reservoir configuration and wellbore distribution used in the verification process.

1- The pressure and pressure derivative, in dimensionless form, are generated analytically for a constant and equal flow rate from the three wellbores using the following dimensionless parameters. They are plotted in Fig. (13). $x_{eD} = 4.0 \quad y_{eD} = 6.0 \quad L_{D1} = L_{D2} = L_{D3} = 60.0 \quad r_{wD} = 0.00033 \quad z_{wD} = 0.5 \quad x_{wD1} = 0.25 \quad y_{wD1} = 3.0$

2- The productivity index for the transient and pseudo-steady state is calculated analytically, in dimensionless form, and plotted in Fig. (13).

3- The dimensionless pressure and pressure derivative, and the productivity index are converted to real-time units and plotted in Fig. (14).

4- The pressure behavior is generated using CMG and compared with the pressure behavior generated analytically as shown in Fig. (15). An excellent matching between the two behaviors is obtained.

5- The starting time of the interference among these three wellbores, represented by developing the early pseudo-steady state flow regime, is determined analytically using the proposed models in this study. It has been found that this time is almost (4.0 days) while from CMG, the starting time of interference is seen after (6.5 days). While the bottom hole pressure drop at which the interference is seen for the first time calculated by both techniques is almost (100 psi). Fig. (16a) shows the starting of the well interference among the three wellbores. A transition flow regime after the first pseudo-steady state flow regime is seen. This flow regime represents the depletion process of reservoir fluids accumulated among wellbores. It lasts for a long time (more than 200 days)

before reaching reservoir boundaries that are normal to the direction of the wellbore and developing pseudo-steady state flow regime completely after reaching all reservoir boundaries.

6- The starting time of pseudo-steady state flow at which the reservoir boundaries have been reached is determined analytically and numerically. It has been found this time is almost (350 days) calculated by the analytical models proposed in this study while it is (430 days) estimated by CMG. The pressure drop at the bottom hole at the starting time of pseudo-steady state flow is (2500 psi). Fig. (16b) shows the starting of pseudo-steady state flow.

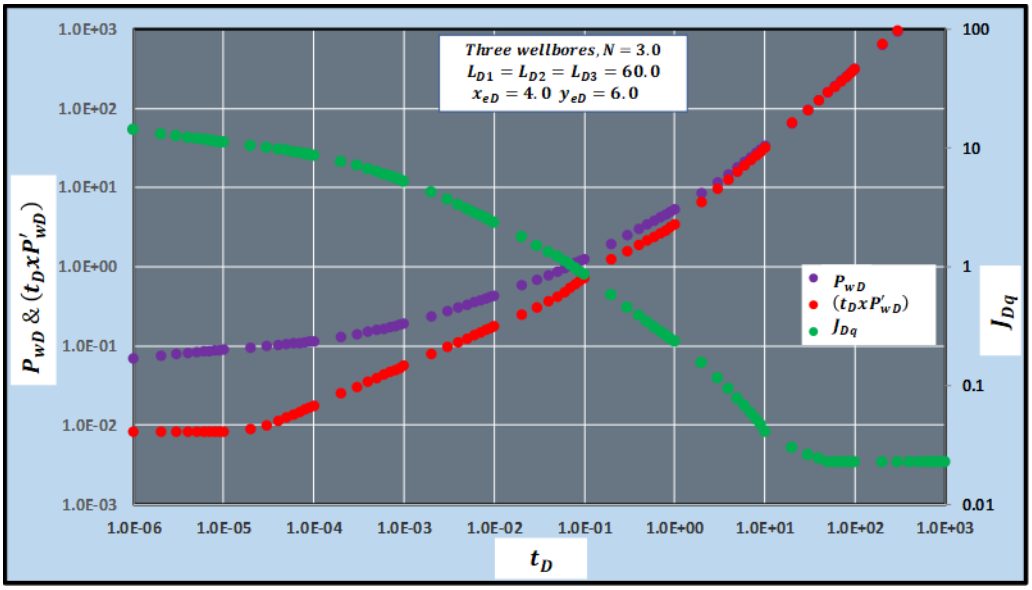

Figure 13: Pressure, pressure derivative, and productivity index behavior in dimensionless form.

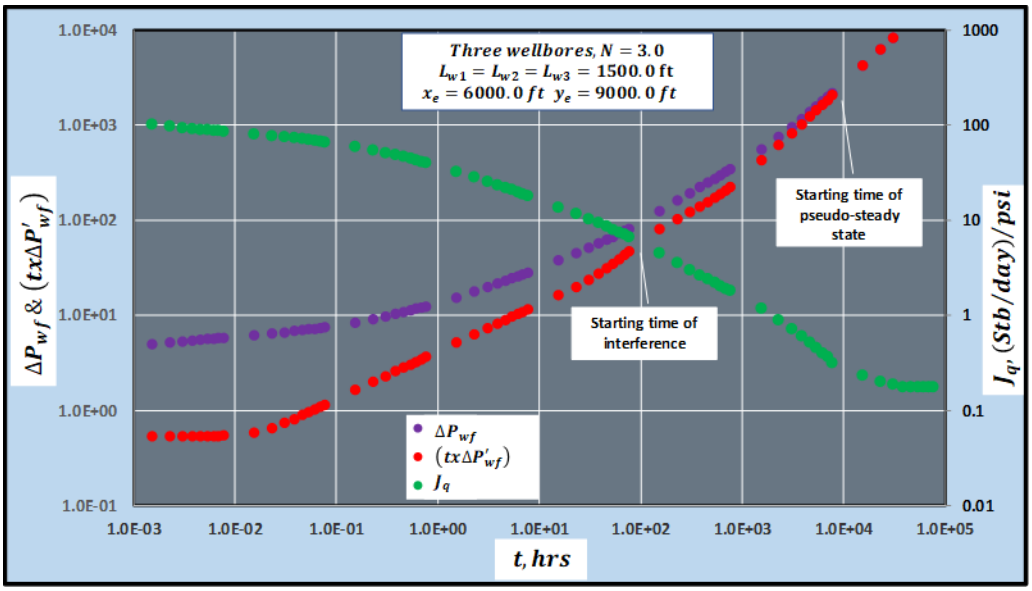

Figure 14: Pressure, pressure derivative, and productivity index behavior in real time units.

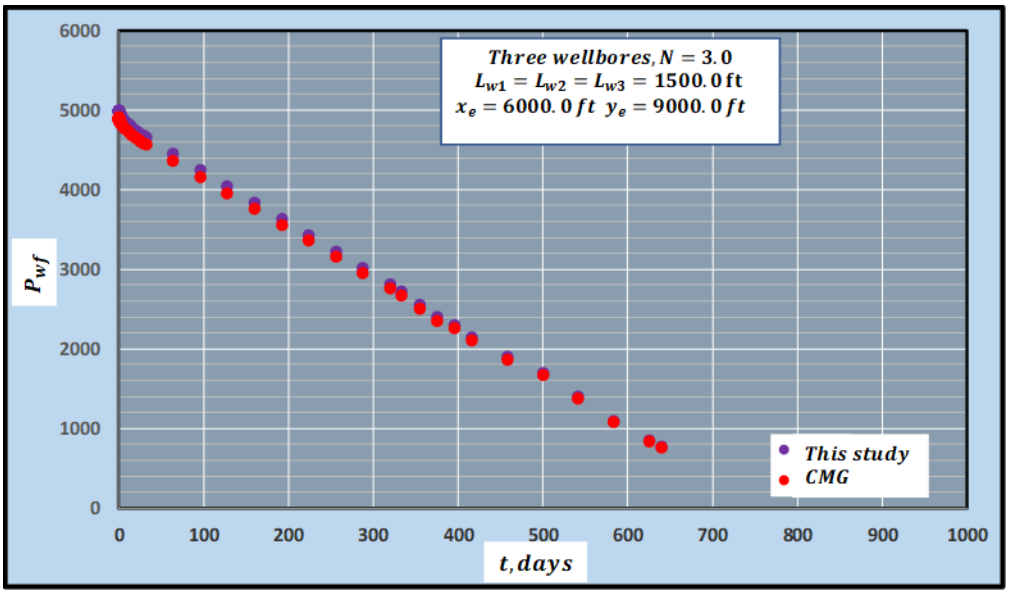

Figure 15: Comparison of bottom hole flowing pressure.

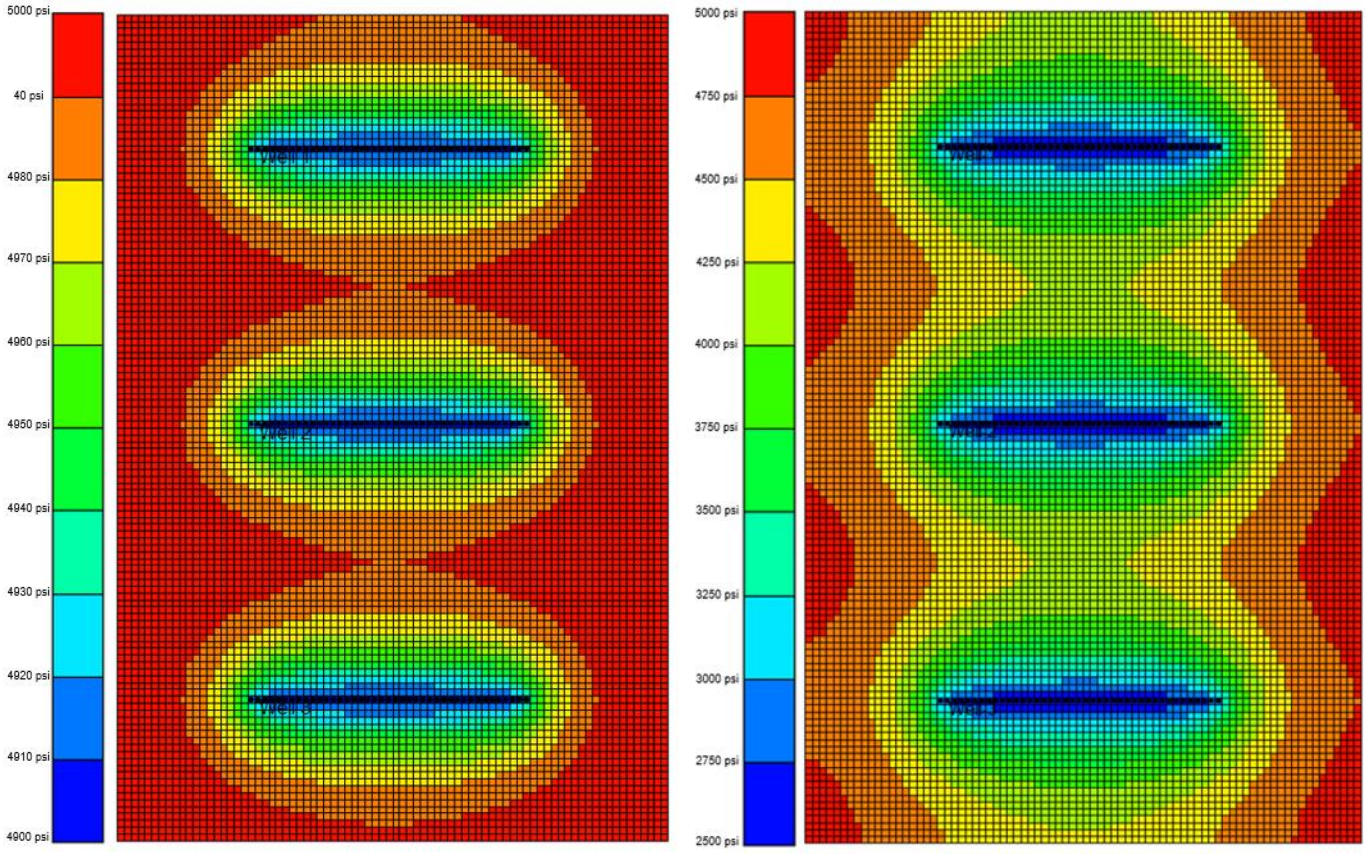

(a) (b)

Figure 16: (a)The starting time of interference (b) The starting time of pseudo-steady state flow.

7. Conclusions

1-Well spacing may have a significant impact on the pressure, flow regimes, flow rate, cumulative production, and productivity index behavior of different reservoir geometry, drainage area size, and wellbore types and distributions. This impact is not seen at early production time but it is very clear when pseudo-steady state flow is reached.

2-The impact of well spacing for the same number of wellbores that are extended in different drainage areas decreases with the size of the drainage area. Increasing the well spacing causes a significant decrease in the pressure drop that in turn leads to increase the productivity index.

3-The impact of well spacing for the same drainage area depleted by different numbers of wellbores increases with the increase of wellbores. Increasing the number of the wellbores causes decreasing the well spacing and thereafter a significant increase in the pressure drop that in turn leads to decrease the productivity index.

4-The interference among wellbores could occur faster when the well spacing is narrow. It can be observed earlier at the circular drainage areas than rectangular drainage areas even though the wellbores are radially distributed for both of them.

5-Early pseudo-steady state flow regime is developed as an indication for the well interference. It represents the impact of the no-flow boundaries between two adjacent wellbores. It is observed after the linear flow regime and before the pseudo-steady state flow regime. It is typically followed by a transition flow regime that represents the depletion process of reservoir fluids accumulated in the porous media among the wellbores.

6-Early pseudo-steady state flow regime may not last for a long time, however, the transition flow regime could last for a long time depending on the well spacing or the size of the porous media between two adjacent wellbores.

7- The productivity index tends to have a stabilized value when the early pseudo-steady state flow regime is developed. However, this value is greater than the value of the stabilized pseudo-steady state productivity index obtained at late production time after the production pulse has reached the reservoir boundaries.

8-Radially distributed wellbores in rectangular reservoirs may have better performance than parallelly distributed wellbores. The symmetrical distribution of these wellbores could perform better than unsymmetrically distributed wellbores.

Nomenclatures

A_D	$Dimensionless\ drainage\ area$
B_o	$Oil\ formation\ volume\ factor$
c_t	$Formation\ total\ compressibility, psi^{-1}$
D_D	$Well\ spacing, dimensionless$
h	$Formation\ thickness, ft$
K_o	$Bessel\ function\ K-type\ of\ zero-order$
K_1	$Bessel\ function\ of\ K-type\ of\ the\ first\ order$
I_o	$Bessel\ function\ of\ I-type\ of\ zero-order$
I_1	$Bessel\ function\ of\ I-type\ of\ the\ first\ order$
k	$Formation\ permeability, md$
k_x	$Formation\ permeability\ in\ X-direction, md$
k_y	$Formation\ permeability\ in\ Y-direction, md$
k_z	$Formation\ permeability\ in\ Z-direction, md$
J_q	$Productivity\ index\ of\ \ constant\ sand\ face\ flow\ rate, (STB/day)/psi$
J_P	$Productivity\ index\ of\ constant\ bottom\ hole\ flowing\ pressure, (STB/day)/psi$
J_{Dq}	$Productivity\ index\ for\ \ constant\ sand\ face\ flow\ rate, dimensionless$
J_{DP}	$Productivity\ index\ of\ constant\ bottom\ hole\ flowing\ pressure, dimensionless$
L_D	$Dimensionless\ wellbore\ length$
L_w	$Half\ wellbore\ length, ft$
N	$Number\ of\ wellbores$
N_D	$Dimensionless\ cumulative\ production$
P_{wf}	$Bottom\ hole\ flowing\ \ pressure\ drop, psi$
P_D	$Pressure\ drop, dimensionless$
P_{wD}	$Bottom\ hole\ flowing\ pressure, dimensionless$
ΔP	$Pressure\ drop, psi$
q	$Flow\ rate, STB/day$

q_t	$Total\ flow\ rate, STB/day$
q_D	$Dimensionless\ flow\ rate$
r	$Radius, ft$
r_D	$Dimensionless\ radius$
r_e	$Reservoir\ radius, ft$
r_{eD}	$REservoir\ radius, dimensionless$
r_w	$Wellbore\ radius, ft$
r_{wD}	$Dimensionless\ wellbore\ radius$
s	$Laplace\ operator$
s_m	$Skin\ factor$
t	$Time, hrs$
t_D	$Time, dimensionless$
T	$Reservoir\ temperature$
$(t_D x P'_D)$	$Pressure\ derivative, dimensionless$
$(t_D x P'_{wD})$	$Bottom\ hole\ flowing\ pressure\ derivative, dimensionless$
$(t x P'_{wf})$	$Bottom\ hole\ flowing\ pressure\ derivative$
x	$X-coordinate\ of\ a\ point\ in\ the\ porous\ media$
x_e	$Reservoir\ boundary, ft$
x_w	$X-coordinate\ of\ a\ wellbore$
x_D	$X-coordinate\ of\ a\ point\ in\ the\ porous\ media, dimensionless$
x_{eD}	$Reservoir\ length, dimensionless$
x_{wD}	$X-coordinate\ of\ a\ wellbore, dimensionless$
y	$Y-coordinate\ of\ a\ point\ in\ the\ porous\ media$
y_e	$Reservoir\ boundary, ft$
y_w	$Y-coordinate\ of\ a\ wellbore$
y_D	$Y-coordinate\ of\ a\ point\ in\ the\ porous\ media, dimensionless$
y_{eD}	$Reservoir\ width, dimensionless$
y_{wD}	$Y-coordinate\ of\ a\ wellbore, dimensionless$
z	$Z-coordinate\ of\ a\ point\ in\ the\ porous\ media$
z_w	$Z-coordinate\ of\ a\ wellbore$
z_D	$Z-coordinate\ of\ a\ point\ in\ the\ porous\ media, dimensionless$
z_{wD}	$Z-coordinate\ of\ a\ wellbore, dimensionless$
μ	$Viscosity, cp$
$\emptyset$	$Porosity$
β	$Non-Darcy\ flow\ coefficient$
γ_g	$Gas\ specific\ gravity$
θ	$The\ deviation\ angle\ in\ the\ horizontal\ plane\ between\ two\ adjacent\ wellbores$

References

[1] Barlow, W. H., & Berwald, W. B., 1945. Optimum Oil-Well Spacing. API (American Petroleum Institute) paper presented at the twenty-fifth annual meeting held in Chicago, IL, USA, SPE 45-129.

[2] Harrison, Rowland, 1970. Regulation of oil and gas production. Alberta Law Review, 8(03). doi.org/10.29173/alr1860

[3] Cutler Jr., Willard W., 1924. Estimation of underground oil reserves by oil-well production curves. Bulletin 228, Bureau of mines, Washington government printing office.

[4] Haseman, W. P., 1930. A Theory of Well Spacing. Society of Petroleum Engineers, transaction of AIME. doi:10.2118/930146-G.

[5] Phelps, R. W., 1929. Analytical Principles of the Spacing of Oil and Gas Wells. Society of Petroleum Engineers, transaction of AIME. doi:10.2118/929090-G.

[6] Foley, L. L., 1938. Spacing of Oil Wells. Society of Petroleum Engineers, transaction of AIME. doi:10.2118/938015-G.

[7] Muskat, M., 1940. Principles of Well Spacing. Society of Petroleum Engineers, transaction of AIME. doi:10.2118/940037-G.

[8] Elliot, G. R., 1951. Well Interference Supports Wide Spacing. API (American Petroleum Institute) paper presented at the Spring meeting of the mid-continent district held in Amarillo, TX, USA

[9] Craze, R.C., 1958. Spacing of Natural Gas Wells. Trans action of AIME, 213 (1958): 213–219. doi.org/10.2118/1056-G

[10] Miller, C. C., and Dyes, A. B., 1959. Maximum Reservoir Worth - Proper Well Spacing. Society of Petroleum Engineers, transaction of AIME, SPE 1217-G.

[11] Heuer, G.J., Clark, G.C., and J.N. Dew, 1961. The Influence of Production Rate, Permeability Variation and Well Spacing on Solution-Gas-Drive Performance. JPT 13 (05). doi.org/10.2118/1519-G-PA

[12] Chacon H., Francisco, 1973. Optimum Well Spacing for the Gas Reservoirs of the Mexican-Republic. Paper presented at the Fall Meeting of the Society of Petroleum Engineers of AIME, Las Vegas, Nevada, Sep. 30-Oct. 3. doi.org/10.2118/4579-MS

[13] Bommer, P., Bayne, M., Mayerhofer, M., Machovoe, M., & Staron, M., 2017. Re-Designing from Scratch and Defending Offset Wells: Case Study of a Six-Well Bakken Zipper Project, McKenzie County, ND. SPE paper presented at the SPE hydraulic fracturing technology conference and exhibition held in Woodland, TX, USA, Jan.24-26. doi:10.2118/184851-MS.

[14] Camacho-Velazquez, R., & Galindo-Nava, A., 1996. Optimum Position for Wells Producing at Constant Wellbore Pressure. SPE Journal, 1 (02), pp.155-168. doi:10.2118/28715-PA.

[15] Valko, P.P., Doublet, L.E., and Blasingame, T.A., 2000. Development and application of the multiwell productivity index (MPI). SPE Journal, 5 (01), pp. 21-31. doi:10.2118/51793-PA.

[16] Umnuayponwiwat, S., Ozkan, E., & Raghavan, R., 2000. Pressure Transient Behavior and Inflow Performance of Multiple Wells in Closed Systems. Paper presented at the SPE Annual technical conference and exhibition held in Dallas, TX, USA, Oct. 1-4.doi:10.2118/62988-MS.

[17] Guo, Boyun, Ghalambor, Ali, and Kegang Ling, 2008. A Rigorous Composite-Inflow-Performance Relationship Model for Multilateral Wells. SPE Production & operation, 23 (02). doi.org/10.2118/100923-PA

[18] He, Dongbo , Jia, Ailin , Jia, Chengye , Guo, Jianlin , and Guang Ji., 2010. Well Spacing Optimization for Tight Sandstone Gas Reservoir. Paper presented at the International Oil and Gas Conference and Exhibition in China, Beijing, China, June 2010. doi.org/10.2118/131862-MS

[19] Wilson, Adam, 2016. Completion and Well-Spacing Optimization for Horizontal Wells in Pad Development. JPT, 68 (10). doi.org/10.2118/1016-0054-JPT

[20] Suarez, M.., and S. Pichon, 2016. Completion and Well Spacing Optimization for Horizontal Wells in Pad Development in the Vaca Muerta Shale. Paper presented at the SPE Argentina Exploration and Production of Unconventional Resources Symposium, Buenos Aires, Argentina, June 2016. doi.org/10.2118/180956-MS

[21] Sahai, V., Jackson, G., Rai, R. R., & Coble, L., 2012. Optimal Well Spacing Configurations for Unconventional Gas Reservoirs. SPE paper at the America's unconventional resources held in Pittsburg, PA, USA, June 5-7.doi:10.2118/155751-MS.

[22] Zhu, J., Forrest, J., Xiong, H., & Kianinejad, A., 2017. Cluster Spacing and Well Spacing Optimization Using Multi-Well Simulation for the Lower Spraberry Shale in Midland Basin. SPE paper presented at the SPE Liquids-Rich Basins Conference-North America held in Midland, TX, USA, Sep. 13-14. doi:10.2118/187485-MS.

[23] Bansal, N., Han, J., Shin, Y., & Blasingame, T., 2018. Reservoir Characterization to Understand Optimal Well Spacing: A Wolfcamp Case Study. SPE paper presented at the unconventional resources technology conference held in Houston, TX, USA. doi:10.15530/URTEC-2018-2901322.

[24] Al-Rbeawi, Salam, 2020. An Approach for the Performance-Impact of Parent-Child Wellbores Spacing and Hydraulic Fractures Cluster Spacing in Conventional and Unconventional Reservoirs. Journal of petroleum science & engineering, 185(2020). doi.org/10.1016/j.petrol.2019.106570

[25] Van Everdingen, A.F., 1949. The application of the Laplace transformation to flow problems in reservoirs. Petroleum Transaction, AIME, 186, pp.305-324. doi:10.2118/949305-G.

[26] Helmy, M. W., & Wattenbarger, R. A.,1998. New Shape Factors for Wells Produced at Constant Pressure. Paper presented at the SPE gas technology symposium held in Calgary, Canada, March 15-18. doi:10.2118/39970-MS.

[27] Ozkan, E. 1988. Performance of horizontal wells. PhD dissertation, The University of Tulsa, Tulsa, Ok, USA.

[28] Ozkan, E., & Raghavan, R., 1991. Some New Solutions to Solve Problems in Well Test Analysis: Part 1 - Analytical Considerations (included associated papers 28626 and 29213). SPE Formation Evaluation, 6 (03), pp. 359-368. doi:10.2118/18615-PA.

[29] Ozkan, E., & Raghavan, R., 1991. Some New Solutions to Solve Problems in Well Test Analysis: Part 2 - Computational Considerations and Applications. SPE Formation Evaluation, 6 (03), pp. 369-378. doi:10.2118/18616-PA.

[30] Wang, X. and Economides, M., 2009. Advanced natural gas engineering. Gulf publishing company, Houston, Texas, USA.

[31] Al-Rbeawi, S. and Artun. E., 2019. Fishbone type horizontal wellbore completion: A study for pressure behavior, flow regimes, and productivity index. JPSE, 176(2019).doi.org/10.1016/j.petro.2018.12.076

[32] MathWorks, 2018, MATLAB and Simulink, Release 2018b, 9.5.0.944444, Natick, Massachusetts, USA.

[33] CMG, 2017, Computer modeling group, Calgary, Alberta, Canada.

Appendix-A: Dimensionless parameters

$$A_D = x_{eD} y_{eD} \; for \; rectangular \; reservoirs \qquad \text{(A-1)}$$

$$A_D = \pi r_{eD}^2 \quad for\ circular\ reservoirs \tag{A-2}$$

$$L_D = \frac{L_w}{h}\sqrt{\frac{k_z}{k}} \tag{A-3}$$

$$P_D = \frac{k\Delta P}{141.2 q \mu B_o} \tag{A-4}$$

$$r_D = \frac{r}{L_w} \tag{A-5}$$

$$r_{eD} = \frac{r_e}{L_w} \tag{A-6}$$

$$r_{wD} = \frac{r_w}{L_w} \tag{A-7}$$

$$t_D = \frac{0.0002637\ kt}{\emptyset \mu c_t L_w^2} \tag{A-8}$$

$$x_D = \frac{x}{x_e} \tag{A-9}$$

$$x_{eD} = \frac{x_e}{L_w}\sqrt{\frac{k}{k_x}} \tag{A-10}$$

$$x_{wD} = \frac{x_w}{x_e} \tag{A-11}$$

$$y_D = \frac{y}{y_e} \tag{A-12}$$

$$y_{eD} = \frac{y_e}{L_w}\sqrt{\frac{k}{k_y}} \tag{A-13}$$

$$y_{wD} = \frac{y_w}{y_e} \tag{A-14}$$

$$z_D = \frac{z}{h} \tag{A-15}$$

$$y_{wD} = \frac{z_w}{h} \tag{A-16}$$

Conversion factors

bbl	x 1.589873	E-01=m^3
cp	x 1.0	E-03=Pa.s
ft	x 3.048	E-01=m
in	x 2.54	E-00=cm
Psi	x 6.894757	E+00=kPa
lbm	x 0.453592	E+00=Kg
md	x 0.9869	E+11=cm^2